FULL TITLE

Cryptic asexual reproduction in *Caenorhabditis* nematodes

SHORT TITLE

Cryptic asexuality in *Caenorhabditis nouraguensis*

AUTHORS

Piero Lamelza[1,2], Janet M. Young[3], Luke M. Noble[4,#a], Arielle Isakharov[2], Meenakshi Palanisamy[2], Matthew V. Rockman[4], Harmit S. Malik[1,3,5], Michael Ailion[1,2]*

AFFILIATIONS

[1]Molecular and Cellular Biology Graduate Program, University of Washington, Seattle, WA, USA

[2]Department of Biochemistry, University of Washington, Seattle, WA 98195, USA

[3]Division of Basic Sciences, Fred Hutchinson Cancer Research Center, Seattle, WA 98109, USA

[4]Department of Biology and Center for Genomics & Systems Biology, New York University, New York, NY 10003, USA

[5]Howard Hughes Medical Institute, Fred Hutchinson Cancer Research Center, Seattle, WA 98109, USA

[#a]Current address: Institut de Biologie, École Normale Supérieure, Centre National de la Recherche Scientifique (CNRS) UMR 8197, Institut National de la Santé et de la Recherche Médicale (INSERM) U1024, Paris, France, F-75005

[*]Corresponding author: mailion@uw.edu

ABSTRACT

Despite potential advantages of asexuality, most animal species reproduce by sex. This suggests that there are barriers that prevent asexuality arising from an obligately sexual ancestor. One such barrier is the transition from haploid to diploid maternal inheritance. Here we report that females of the normally sexual species *Caenorhabditis nouraguensis* can produce offspring asexually by sperm-dependent parthenogenesis (also called gynogenesis or pseudogamy) in two contexts: (1) when crossed to males of their sister species *C. becei*, or (2) when crossed to UV-irradiated males of their own species. We found that crosses between *C. nouraguensis* females and *C. becei* males result in two classes of viable offspring. The first class consists of fertile offspring, which are produced asexually by gynogenesis; these progeny inherit a diploid maternal genome but fail to inherit a paternal genome. The second class consists of sterile hybrid offspring, which inherit both a diploid maternal genome and a haploid paternal genome. Using whole-genome sequencing of individual viable worms, we show that diploid maternal inheritance results from an altered meiosis in *C. nouraguensis* oocytes and the inheritance of two randomly selected homologous chromatids. This genetic mechanism of diploid maternal inheritance is indistinguishable from that of many obligately asexual species. Thus, *C. nouraguensis* may provide a genetically tractable model to study the evolutionary origins of asexuality from obligately sexual species.

AUTHOR SUMMARY

Eukaryotes employ two major reproductive strategies: sexual and asexual reproduction. Both reproductive modes have potential costs and benefits, and being able to switch between the two may be the optimal reproductive strategy. Indeed, most unicellular eukaryotes can switch between sexual and asexual reproduction. However, most multicellular eukaryotes are obligately sexual, implying that there are barriers blocking the evolution of asexuality from a sexual ancestor. These barriers are largely unknown due to few known transitional forms between sexual and asexual reproduction. We have discovered that the females of a predominantly sexual nematode species can reproduce asexually at a low frequency. This asexual reproduction involves the unusual production of eggs carrying two sets of maternal chromosomes and the loss of the paternal set of chromosomes. We hypothesize that the low-frequency asexual reproduction in this species represents a transitional state between sexual and asexual reproduction, and may serve as a model to understand the barriers to the evolution of asexuality.

Keywords: gynogenesis, asexual, *Caenorhabditis*, automixis, central fusion, paternal genome loss, hybrid, large X-effect, single-worm sequencing

INTRODUCTION

Theory predicts that facultative sex, the ability to undergo both asexual and sexual reproduction, is the optimal reproductive strategy [1–4]. Advantages of asexuality include an immediate two-fold enhancement of fitness and an enhanced ability to disperse geographically by obviating the requirement of a mate for reproduction [5,6]. By contrast, advantages of sexual reproduction include the production of genotypic diversity that could be used to adapt to a changing environment and the ability to purge deleterious alleles through recombination [7]. Most unicellular eukaryotes undergo facultative sex, taking advantage of their ability to switch reproductive strategies as conditions dictate [8,9]. However, most animal species are obligately sexual, suggesting that there must be strong selective pressures to prevent the origin or persistence of asexuality from an obligately sexual ancestor [4]. A better understanding of these selective pressures requires understanding how asexuality evolves from a sexual ancestor. However, very few such transitions are known, and even fewer occur in genetically tractable organisms.

Here we focus on one key aspect of how asexuality evolves from sexually reproducing organisms: diploid maternal inheritance. Sexual reproduction requires that diploid females and males generate haploid eggs and sperm, which then fuse to produce the next generation of diploid offspring. By contrast, asexual females produce diploid eggs that either develop independently of sperm fertilization, known as parthenogenesis [10], or require fertilization but do not inherit the paternal genome, known as gynogenesis or pseudogamy [11]. Thus, understanding how egg production can be modified to result in diploid maternal inheritance should provide insight into how asexuality arises.

There are several known mechanisms of generating diploid eggs in asexual species. In apomixis, eggs produced by mitotic rather than meiotic divisions result in offspring that are clones of their mother. By contrast, automixis maintains the first steps of meiosis, but generates diploid

eggs either by combining two haploid products of meiosis or duplicating one of the four meiotic products [10]. Apomictic (mitotic) parthenogenesis maintains heterozygosity across the entire genome and prevents inbreeding depression, whereas automictic parthenogenesis, via duplication of a single meiotic product, results in genome-wide homozygosity and inbreeding depression. Thus, different mechanisms of generating diploid eggs to establish new asexual lineages can have a range of genetic consequences that influence their success [12].

Interestingly, in some predominantly sexual invertebrate and vertebrate species, females can reproduce asexually at a low frequency [13–20]. Supporting the hypothesis that rare asexuality is an intermediate step in the transition between sexual and asexual reproduction [19,20], genetic studies indicate that rare asexual offspring inherit a diploid maternal genome by mechanisms like those of obligately asexual species. For example, detailed genetic and cytological studies in several sexual *Drosophila* species show that their rare parthenogenetic offspring inherit a diploid maternal genome by automixis [15,21–23]. Furthermore, the frequency of rare parthenogenesis in some *Drosophila* species can be increased through experimental laboratory selection [13,22,24], suggesting that rare asexuality could be a transition step en route to obligate asexuality. However, other than *Drosophila*, most sexual species that produce rare asexual offspring are not model organisms. As a result, genetic studies in these non-model species have been typically limited to a handful of genetic markers. Although highly informative, these studies have not revealed sufficient mechanistic insights into the basis of diploid maternal inheritance.

Here we report that a cross between two sexual *Caenorhabditis* nematode species results in rare viable progeny that are fertile or sterile. Fertile offspring are generated by gynogenesis (sperm-dependent parthenogenesis), whereas sterile offspring are hybrids. Both fertile and sterile offspring inherit a diploid maternal genome by automixis, specifically the inheritance of two homologous chromatids. We also find that intraspecific crosses within one of the species, *C.*

nouraguensis, can result in a low frequency of gynogenetic reproduction. Thus, *C. nouraguensis* may represent a nascent asexual lineage.

RESULTS

Reciprocal *C. nouraguensis* x *C. becei* crosses exhibit distinct F1 embryonic lethal phenotypes

C. nouraguensis and *C. becei* are obligately outcrossing sister species consisting of female and male individuals (Fig 1A). We initially studied the hybridization of *C. nouraguensis* strain JU1825 with *C. becei* strain QG711. The mating of individuals within the same strain results in a high proportion of viable progeny (Fig S1, Videos S1 and S2). However, mating *C. becei* females (QG711) to *C. nouraguensis* males (JU1825) results in 100% embryonic death with a stereotypical arrest at approximately the 32-cell stage (Fig 1B, Video S3). In the reciprocal cross between *C. nouraguensis* females (JU1825) and *C. becei* males (QG711), most F1 embryos also die, but some embryos arrest early in development (approximately 1-4 cell stage) whereas some arrest at later stages (approximately 44-87 cell stage) (Video S4).

Crossing *C. nouraguensis* females to *C. becei* males results in rare viable F1 progeny

Interestingly, a small fraction of F1 progeny from *C. nouraguensis* female x *C. becei* male crosses develop into viable adults. Such viable progeny were found using three different *C. nouraguensis* strains and two *C. becei* strains (Fig S2), indicating that the production of viable progeny is a general feature of *C. nouraguensis* female x *C. becei* male crosses. By contrast, no surviving F1 were found in the reciprocal *C. becei* female x *C. nouraguensis* male crosses or crosses between *C. nouraguensis* females and males of other closely related *Caenorhabditis* species (Fig 1B and Fig S2). Thus, production of viable F1 progeny is specific to the *C. nouraguensis* female x *C. becei* male cross. We tested the fertility of each viable F1 animal and found that ~2/3 of F1 were sterile and ~1/3 were fertile (JU1825 x QG711: 18 sterile, 8 fertile; NIC54 x QG711: 27 sterile, 10 fertile) (Fig 1D).

We next tested if the rare viable F1 were indeed interspecies hybrids. We genotyped each F1 at one of two autosomal loci using PCR-restriction digest assays that distinguish between *C. nouraguensis* and *C. becei* alleles (Fig 1C). We found that about two-thirds of viable F1 inherited both parental alleles and therefore are genetic hybrids (JU1825 x QG711: 17/26 F1; NIC54 x QG711: 26/37 F1). However, to our surprise, we found that the remaining viable F1 adults carry only the maternal *C. nouraguensis* allele and no paternal *C. becei* allele (JU1825 x QG711: 9/26 F1; NIC54 x QG711: 11/37 F1) (Fig 1D). Interestingly, all fertile F1 had only the maternal *C. nouraguensis* allele and not the paternal *C. becei* allele, while all but two sterile F1 had a hybrid genotype with alleles from both parents. We observed a similar correlation between genotype and fertility among rare viable F1 animals when a different paternal *C. becei* strain was used (Fig S3).

Interspecies hybrids are often sterile [25], but it was surprising to find fertile F1 that inherited only maternal *C. nouraguensis* DNA. These fertile F1 behave like *C. nouraguensis* when backcrossed to either parental species. Backcrossing fertile F1 to *C. nouraguensis* results in many viable F2 progeny that develop to adulthood. By contrast, backcrossing fertile F1 to *C. becei* results in almost all F2 dying during embryogenesis other than the few rare viable F2 progeny in crosses to *C. becei* males (as in the original interspecies cross). Thus, it appears that interspecies hybridization between *C. nouraguensis* females and *C. becei* males produces a low frequency of fertile F1 that carry only maternal *C. nouraguensis* DNA.

One way *C. nouraguensis* females might produce fertile F1 progeny with a maternal genotype would be to generate sperm and reproduce as hermaphrodites at a low frequency. To test this possibility, we monitored 60 virgin females from two *C. nouraguensis* strains (JU1825 and NIC59) and two *C. becei* strains (QG704 and QG711) for five days but failed to find any progeny. Thus, production of fertile F1 is not due to cryptic hermaphroditism but requires mating to *C. becei* males. We hypothesize that fertile F1 are the result of gynogenetic reproduction in which *C.*

nouraguensis oocytes require fertilization by *C. becei* sperm to initiate development, but do not inherit the paternal *C. becei* genome.

Fertile interspecific F1 females are diploid

How do the fertile F1 compensate for the lack of a paternal haploid genome? We presumed that the autosomes of the fertile F1 had to be at least diploid for viability because haploid *C. elegans* individuals die during embryogenesis [26], and all well-studied *Caenorhabditis* species have five diploid autosomes and an X chromosome that is either diploid (females) or haploid (males) [27–29].

We determined the ploidy of fertile F1 females by counting the number of chromosomes in their oocytes. In *C. elegans*, the female germline produces oocytes containing chromosomes that have undergone prophase of meiosis I (DNA replication and recombination) but have yet to undergo the two meiotic divisions. The oocyte contains six bivalents, each of which is composed of a pair of homologous chromosomes and their sister chromatids held together by a combination of recombination and sister chromatid cohesion (Fig 2A). Therefore, diploid individuals have six bivalents in their oocytes, which appear as six distinct DAPI-staining bodies (Fig 2B). In *C. elegans*, meiotic recombination occurs only once per homologous set of chromosomes [30]. Thus, a triploid individual will have two homologous chromosomes that recombine and form a bivalent as well as a non-recombinant homolog as a univalent. Therefore, triploid individuals have six bivalents and six univalents in mature oocytes, which appear as twelve DAPI-staining bodies (Fig 2B) [31].

We crossed *C. nouraguensis* (JU1825) females to *C. becei* (QG711) males, collected fertile F1 females and dissected and stained their germlines with DAPI. As controls, we examined the germlines of JU1825 and QG711 females after mating with conspecific males. Both parental species mostly have six DAPI-staining bodies, consistent with six diploid chromosomes (like *C.*

elegans). Most fertile F1 females also have six DAPI-staining bodies, indicating they are diploid (Fig 2C and Fig S4).

Fertile interspecific F1 inherit two random homologous chromatids from each maternal *C. nouraguensis* bivalent

There are three mechanisms by which the fertile F1 animals could result from diploid maternal inheritance. They could inherit two chromatids from each maternal bivalent in a *C. nouraguensis* oocyte, inherit one chromatid from each bivalent and undergo genome-wide diploidization by endoreplication, or inherit the original two maternal chromatids by producing diploid eggs by mitosis (apomixis). To distinguish between these possibilities, we used whole-genome sequencing of individual worms to determine the genetic identity of the chromatids inherited by fertile F1 individuals.

All four of the chromatids within a bivalent are genetically distinct; of the six possible ways of combining two chromatids, four have distinct chromosomal genotypes and two are indistinguishable by Illumina whole-genome sequencing (Fig 3A, 3B and Fig S5A). Thus, the genotype of the fertile F1 can indicate which two chromatids were inherited. Because recombination in *Caenorhabditis* species occurs predominantly on chromosome arms [32,33], inheriting two sister chromatids would usually result in homozygosity in the centers of chromosomes and heterozygosity on one of the arms, whereas inheriting two homologous chromatids would result in heterozygosity in the center of each chromosome (Fig 3B). By contrast, endoreplication of single chromatids would lead to homozygosity along all chromosomes, and apomixis would lead to heterozygosity along all chromosomes (Fig S6).

We first crossed two genetically distinct *C. nouraguensis* strains, NIC59 and JU1825, to generate heterozygous *C. nouraguensis* (NIC59/JU1825) females, which we then crossed to *C. becei* (QG711) males. We collected eleven fertile F1 and performed whole-genome amplification

and sequencing of each one (Fig 3A). We determined the genotype of each fertile individual's chromosomes by calculating average NIC59 SNP frequencies in 50-kb windows across their genome (see Materials and Methods for details). An approximately 0.50 NIC59 allele frequency was inferred as heterozygosity (NIC59/JU1825), whereas an approximately 1.0 or 0.0 NIC59 allele frequency was inferred as homozygous NIC59 or JU1825, respectively. This experiment also allowed us to determine whether fertile F1 inherit only maternal *C. nouraguensis* DNA or whether some paternal *C. becei* DNA is also present.

We found that nearly 100% of each fertile F1's reads map to the *C. nouraguensis* genome assembly; only a small percentage (0.1-0.2%) map to the *C. becei* genome assembly (Table S1 and Fig S7). These results resemble our controls that contain only *C. nouraguensis* DNA (samples: F1_NIC59_JU1825 and NIC59plusJU1825, Table S1 and Fig S7). Therefore, our sequencing results confirm that fertile F1 inherit only maternal *C. nouraguensis* DNA. Strikingly, whole-chromosome genotyping data shows that the fertile F1 always inherited two homologous chromatids from each maternal bivalent (Fig 3C, Fig S5 and Fig S7). Combining chromosome genotypes from the fertile F1 indicates that two randomly selected homologous chromatids were inherited (Fig 3D). Based on these findings, we can rule out endoreplication and apomixis. Instead, we conclude that diploid, fertile F1 inherit two homologous chromatids from each maternal bivalent in *C. nouraguensis* oocytes.

Sterile F1 inherit a diploid *C. nouraguensis* genome and a haploid *C. becei* genome

Having established that fertile F1 adults inherit only a diploid maternal genome, we next examined the genome-wide inheritance pattern in sterile F1 adults. We performed whole-genome sequencing of ten sterile F1 adults derived from the same interspecies crosses mentioned in the previous section (Fig 3A).

Surprisingly, five of the sterile F1 appear to be triploid hybrids that inherited a diploid *C. nouraguensis* maternal genome and a haploid *C. becei* paternal genome (females F1_6, F1_12, F1_20; males F1_17 and F1_21, Table S1). In these individuals, the normalized coverage of *C. nouraguensis* autosomes was approximately double that of the *C. becei* autosomes (Fig 4A). Furthermore, genotyping of the *C. nouraguensis* chromosomes revealed that these individuals inherited two homologous chromatids from each maternal *C. nouraguensis* bivalent, just like the fertile F1 (Fig 4B and Fig S7). Three other sterile F1 males are also hybrids that inherited two homologous chromatids from each maternal bivalent. However, they are unlikely to be true, full triploids because the normalized coverage of the *C. becei* autosomes is considerably less than half that of the *C. nouraguensis* autosomes (males: F1_10, F1_16 and F1_23, Fig 4A). Instead, we hypothesize that the reduced coverage of the *C. becei* genome results from mosaicism, in which only a subset of cells in these individuals contain the paternal *C. becei* DNA. The *C. becei* autosomes within each individual hybrid mosaic exhibit similar levels of coverage (except perhaps Chr. V of F1_16), suggesting that most hybrid cells within these individuals have a complete haploid copy of the *C. becei* autosomal genome (diploid-triploid mosaic hybrids) (Fig 4A).

Combining maternal chromosome genotypes from the sterile F1 indicates that two randomly selected homologous chromatids were inherited (Fig 4C and Fig S5C). Additionally, the combined data on maternal genotype frequencies from both sterile and fertile F1 also indicate random homologous chromatid inheritance (Fig 4D and Fig S5C). These results show that both the fertile and sterile F1 share the same mechanism of diploid maternal inheritance and are distinguished by whether they inherited the haploid *C. becei* genome.

The *C. becei* X-chromosome is toxic to F1 hybrids

In *Caenorhabditis*, males are hemizygous for the X-chromosome (XO) and produce haploid sperm that carry either a single X or no X. Therefore, roughly half of the F1 are expected to inherit

the paternal *C. becei* X-chromosome. However, despite inheriting *C. becei* autosomes, none of the sterile F1 we sequenced show inheritance of the *C. becei* X-chromosome (Fig S7). We collected additional viable F1 hybrids from the interspecies cross and determined whether any inherited the *C. becei* X-chromosome by PCR genotyping of two indel polymorphisms, one X-linked and one autosomal, that distinguish between *C. nouraguensis* and *C. becei* sequences (Fig 5A). We found that none of the F1 inherited the *C. becei* X-chromosome (Fig 5B), regardless of whether they were autosomal hybrids (22 females and 12 males) or had a maternal genotype (10 females).

Our failure to find any viable F1 carrying a *C. becei* X-chromosome suggests that it is toxic to F1 hybrids. Alternatively, this pattern could reflect an unusual segregation pattern specifically involving the X chromosome in hybrids. To distinguish between these possibilities, we PCR genotyped dead F1 embryos from the same interspecies cross. Consistent with the expected inheritance of the X-chromosome from males, we found that 17 of 34 (50%) dead F1 embryos inherited both the *C. becei* paternal X-chromosome and the *C. nouraguensis* maternal X-chromosome, whereas 16 of 34 (47%) inherited only the maternal *C. nouraguensis* X-chromosome (Fig 5B). One dead F1 embryo possessed only a paternal *C. becei* genotype, suggesting that it lost the maternal *C. nouraguensis* X-chromosome. Because dead F1 embryos can inherit the *C. becei* X-chromosome but viable F1 animals do not, we conclude that the *C. becei* X-chromosome is toxic to F1 hybrids. Previous work has described the “large X-effect” on hybrid inviability and sterility [25]. We hypothesize that a dominant incompatibility involving one or more loci on the *C. becei* X chromosome underlies its toxic effect on hybrids with *C. nouraguensis*.

Dead F1 embryos have unusual maternal and paternal inheritance

To determine whether the unusual patterns of maternal and paternal inheritance seen in viable F1 also occur in the dead F1 embryos in the interspecies cross, we PCR genotyped the same dead F1 embryos described above at an autosomal indel polymorphism that distinguishes

the two species (Fig 5C). We found that 27 of the 35 dead F1 embryos (77%) had a heterozygous *C. nouraguensis*/*C. becei* genotype while eight (22%) had an only-maternal *C. nouraguensis* genotype (Fig 5C). These data suggest that although most embryos inherit both maternal and paternal DNA, a significant fraction fail to inherit paternal *C. becei* DNA for this marker. Aneuploidy caused by incomplete loss of the paternal genome may contribute to death of embryos.

To determine whether dead F1 embryos also inherit two homologous *C. nouraguensis* chromatids from each maternal bivalent, we PCR genotyped them at an autosomal indel polymorphism in the center of chromosome I that distinguishes NIC59 and JU1825 alleles. We found that 34 of 36 dead F1 embryos had a heterozygous NIC59/JU1825 genotype, whereas one embryo had a JU1825 genotype and one embryo had a NIC59 genotype (Fig 5D). These data suggest that very few embryos are derived from a canonical female meiosis in which a haploid maternal complement is inherited. Instead, most embryos appear to have inherited two homologous chromatids from an aberrant female meiosis.

To better understand how female meiosis is modified so that at least two homologous chromatids are inherited, we quantified the number of polar bodies found in F1 embryos, of which the vast majority are expected to die. If most *C. nouraguensis* oocytes fertilized by *C. becei* sperm have aberrant meiotic segregations that result in the inheritance of two homologous chromatids, we would predict that fewer than two polar bodies are formed. We DAPI stained F1 embryos derived from crossing *C. nouraguensis* (NIC59) females to *C. becei* (QG711) males. As a control, we stained embryos derived from intraspecies NIC59 crosses. As expected, NIC59 embryos almost always have two polar bodies whose morphology and size appear similar across individuals (Fig 5E and 5I). Interestingly, we found that 2/90 NIC59 embryos had only one polar body (Fig 5F and 5I), suggesting that abnormal meiosis can occur at a low frequency in intraspecies crosses. By contrast, approximately half of the hybrid embryos have only one polar body (52/102), probably indicating that one of the two female meiotic divisions has failed (Fig 5G-I). The polar bodies in

hybrid embryos can also appear abnormal in their morphology (Fig 5I). Together with our genotyping data, these observations indicate that meiotic segregations are frequently perturbed in *C. nouraguensis* females mated to *C. becei* males.

Hybrid embryos inherit sperm centrioles and DNA, but exhibit mitotic defects

During fertilization in *Caenorhabditis,* the sperm deposits centrioles and a condensed paternal genome into the egg where it forms a pronucleus (Fig 6A). The paternal pronucleus then decondenses and migrates to join the maternal pronucleus for the first mitotic division (Fig 6B-E) [34]. In obligately gynogenetic species, the paternal genome can be lost by remaining condensed during the first few mitotic divisions of the zygote rather than being replicated and segregated properly [35,36]. To determine whether paternal genome loss in hybrid embryos is similar to that of obligately gynogenetic species, we stained *C. nouraguensis* x *C. becei* F1 hybrid embryos with DAPI (staining DNA) and antibodies to α-tubulin (staining spindles) and γ-tubulin (staining centrosomes). We found that hybrid embryos always have centrioles and a paternal genome derived from the sperm as is normal in *Caenorhabditis*, but in a small fraction of animals, the centrioles are abnormally dissociated from the male pronucleus (Fig 6I and 6M). We consistently observed both paternal and maternal pronuclei decondensing and meeting (Fig 6M). Thus, paternal genome loss in hybrid embryos does not appear to result from a failure of the paternal pronucleus to decondense, suggesting that the paternal DNA is lost later in development.

We also observed later stages of hybrid embryogenesis from metaphase of the first mitosis to the four-cell stage. We found that a fraction of hybrid embryos exhibit DNA that is not properly aligned on the mitotic spindle (Fig 6J and 6M), lagging DNA during or after anaphase (Fig 6K and 6M), and probable micronuclei during interphase (Fig 6L and 6M). Although it is unclear whether the aberrant DNA is maternal or paternal, the data are consistent with paternal genome loss at later embryonic stages.

Diploid maternal inheritance occurs occasionally in *C. nouraguensis* intraspecies crosses

To determine whether diploid inheritance from *C. nouraguensis* oocytes can occur independently of interspecies hybridization, we designed an experiment in which *C. nouraguensis* sperm can fertilize *C. nouraguensis* oocytes but do not contribute the paternal genome. In this scenario, a canonical female meiosis would result in haploid maternal genome inheritance and the embryos would fail to develop into viable adults [26]. However, if *C. nouraguensis* oocytes inherit a diploid maternal genome, they could complete embryogenesis and develop into viable adults.

We blocked the inheritance of the haploid sperm genome using UV irradiation to damage and inactivate the sperm genome while still allowing for fertilization and development of the maternal haploid embryo [37,38]. We exposed NIC59 and JU1825 adult males to a high dose of shortwave UV radiation and then crossed them to unexposed JU1825 or NIC59 adult virgin females, respectively. We then screened for and PCR genotyped viable progeny at several autosomal loci to determine whether they inherited both maternal and paternal DNA (heterozygous NIC59/JU1825) or just maternal DNA (Fig 7A).

From a cross of JU1825 females to NIC59 UV-irradiated males, only seven out of approximately 18,000 embryos survived to adulthood. Upon PCR genotyping a chromosome I indel polymorphism, we found that four of these seven individuals had a heterozygous NIC59/JU1825 genotype and therefore inherited both maternal and paternal alleles at this locus. We presume these animals represent rare cases in which the sperm genome was not destroyed. However, three females inherited only the maternal JU1825 allele (Fig 7B). We PCR genotyped these females at two other unlinked autosomal indel polymorphisms. All had a maternal JU1825 genotype at all three loci, suggesting that they inherited only the maternal genome (Fig 7C). We performed similar experiments with NIC59 females and UV-irradiated JU1825 males. Only two out of roughly 7,000 progeny survived to adulthood. These two females had only-maternal NIC59

genotypes at all three autosomal loci (Fig 7B and 7C). We performed additional UV-experiments to better quantify the frequency of gynogenetically-produced offspring. In total, we found that gynogenetically-produced offspring occur at a rate of ~0.01% in JU1825 female x NIC59 male UV crosses and ~0.1% in NIC59 female x JU1825 male UV crosses. Interestingly, each cross had a single gynogenetically-produced male (Fig 7D).

We then determined the ploidy of the gynogenetically-produced females from the UV experiments by counting the number of DAPI-staining bodies in their -1 oocytes. We found that almost all had six DAPI-staining bodies, indicating that they result from diploid maternal inheritance (Fig 7E). The genotyping and DAPI staining data together indicate that diploid maternal inheritance in *C. nouraguensis* oocytes does not require fertilization by *C. becei* sperm and can occur even in intraspecies crosses, at least when the males are sterilized by UV.

A caveat to the UV experiments is that they may not be indicative of what occurs during normal non-irradiated intraspecies crosses. For instance, diploid maternal inheritance could be artificially induced by fertilization with UV-damaged sperm. To determine whether female meiosis is perturbed when oocytes are fertilized by UV-irradiated sperm, we stained embryos derived from JU1825 female x NIC59 male UV crosses. We found that these embryos always exhibited two superficially normal polar bodies, much like the non-UV control (Fig 7F-H). This result suggests that female meiosis is usually normal when an oocyte is fertilized by UV-damaged sperm. Furthermore, PCR genotyping of dead embryos derived from crossing heterozygous NIC59/JU1825 females to NIC59 UV-irradiated males is consistent with haploid maternal inheritance and destruction of the paternal NIC59 genome (Fig S8). Therefore, our data suggest that female meiosis is not generally perturbed by fertilization with UV-irradiated sperm, and that the diploid maternal inheritance seen in intraspecies crosses is not an artificial byproduct of a grossly disrupted meiosis. In support of this, we observe occasional embryos derived from normal

intraspecies crosses with only a single polar body (Fig 5F and 5I, and Fig 7H), consistent with diploid maternal inheritance occurring independently of UV-irradiation.

DISCUSSION

In this study we investigated the hybridization of two sexual *Caenorhabditis* species, *C. nouraguensis* and *C. becei*. We found that rare viable offspring are produced in the cross of *C. nouraguensis* females to *C. becei* males. About one-third of the viable offspring are fertile and result from a combination of diploid maternal inheritance and paternal genome loss, two traits that define gynogenetic reproduction. The remaining viable offspring are sterile and possess a diploid maternal *C. nouraguensis* genome and a haploid paternal *C. becei* genome. However, none of the sterile hybrids inherit the *C. becei* X-chromosome, although it is inherited at the expected frequency in dead embryos. Furthermore, we find evidence that one of the two female meiotic divisions consistently fails in the dead hybrid embryos, and these embryos also inherit two homologous maternal chromosomes, like the viable offspring. Finally, we found that diploid maternal inheritance also occurs at a low frequency in intraspecies *C. nouraguensis* crosses, as revealed by UV-irradiation of males. These data suggest that the same mechanism of diploid maternal inheritance occurs in both intraspecies and interspecies crosses, but that the low-frequency diploid maternal inheritance inherent to *C. nouraguensis* oocytes is drastically increased when they are fertilized by *C. becei* sperm. This suggests that a signal from *C. becei* sperm alters *C. nouraguensis* female meiosis.

Mechanism of diploid maternal inheritance

We found that diploid maternal inheritance in fertile and sterile offspring almost always results from inheriting two randomly selected homologous chromatids from each maternal bivalent in the oocyte. We hypothesize that this diploid maternal inheritance reflects a stereotypical segregation mechanism that is a slight modification of canonical meiotic divisions (Fig 8A).

One way to inherit a diploid maternal genome would be the failure of the second meiotic division. However, this mechanism would result in the oocyte inheriting two sister chromatids rather

than two homologous chromatids and therefore does not account for the gynogenetic development observed in *C. nouraguensis*. Instead, we propose that gynogenetic development in *C. nouraguensis* results from an alteration of the first meiotic division followed by a normal second meiotic division. In our model (Fig 8B), meiotic prophase occurs normally in *C. nouraguensis* oocytes, generating six recombinant bivalents. Upon fertilization by *C. becei* sperm, homologs segregate normally at anaphase I. However, instead of segregating one set of homologs into the first polar body, both sets are retained in the oocyte. Both half-bivalents within the oocyte then randomly segregate sister chromatids at anaphase II. One chromatid segregates into a polar body while the other is retained in the oocyte. Thus, the oocyte inherits two randomly selected homologous chromatids from each bivalent. This model suggests that diploid maternal inheritance could result from a modification of female meiosis such as failure of cytokinesis after anaphase I. There is cytological evidence that incomplete anaphase I and a failure of cytokinesis generates diploid eggs in *Daphnia pulex*, which undergoes obligate parthenogenesis [39]. A slightly more complicated model would be that the first meiotic division and polar body formation are normal, but then the chromosomes in the first polar body are reabsorbed into the oocyte and undergo a normal second meiotic division.

Importantly, our model predicts the formation of only one polar body. Approximately half of the dead hybrid embryos have only one polar body (Fig 5G and 5I). Combined with the fact that dead hybrid embryos also inherit two maternal homologs (Fig 5D), our data suggest they also undergo the same mechanism of diploid maternal inheritance. Gynogenetically produced offspring from intraspecies *C. nouraguensis* UV experiments are diploid, but it is currently unclear how their diploidy is attained. However, because embryos from normal *C. nouraguensis* intraspecies crosses have only one polar body on rare occasions (Fig 5F and 5I, and Fig 7H), diploidy in intraspecies crosses may also be attained by a failure of one of the female meiotic divisions.

Some loss-of-function mutations and gene knockdowns in *C. elegans* can possibly lead to diploid maternal inheritance [41,42], suggesting plausible cellular mechanisms underlying this phenomenon. During normal meiosis I in *C. elegans*, the meiotic spindle migrates and orients perpendicularly to the oocyte cortex. In anaphase I, one set of homologs segregates towards the cortex into the first polar body while the other is retained in the oocyte. However, weak knockdown of dynein heavy chain (*dhc-1*) causes the meiotic spindle to be oriented parallel to the cortex rather than perpendicular during meiosis I; as a result, homologous chromosomes segregate parallel to the cortex in anaphase I and no polar body is formed [42]. The half-bivalents that remain in the oocyte then segregate relatively normally during anaphase II and form a polar body. The oocyte presumably inherits two randomly selected homologous chromatids from each bivalent. A similar misalignment of the meiotic spindle at metaphase I is also thought to be the mechanism underlying the generation of diploid eggs in the obligately parthenogenetic species *Drosophila mangabeirai* [43]. We hypothesize that a misalignment of the meiotic spindle or a failure of cytokinesis may similarly result in diploid maternal inheritance in *C. nouraguensis*.

Paternal genome loss

In addition to diploid maternal inheritance, gynogenesis also requires paternal genome loss. In viable F1 offspring from the *C. nouraguensis* x *C. becei* cross, we found that the entire haploid *C. becei* paternal genome can be inherited in all cells (triploid hybrids), only a subset of cells (diploid-triploid mosaic hybrids), or in no cells (fertile gynogenetic offspring). Interestingly, the offspring of naturally gynogenetic fish species can have a similar spectrum of paternal inheritance. Specifically, most offspring completely fail to inherit the paternal genome (diploid maternal clones), but a small fraction of offspring can inherit it in a subset of cells (diploid-triploid mosaic) or all cells (triploid) [35,44,45]. Given these similarities, the mechanism of paternal genome loss in *C. nouraguensis* interspecies gynogenesis might be similar to that of some obligately gynogenetic fish

species. However, paternal genome loss can occur in a variety of contexts and has different underlying causes, each of which could potentially explain the loss of the *C. becei* genome [46–51]. In the context of interspecies hybridization, detailed studies in *Hordeum* (barley) and *Xenopus* show that paternal chromosomes fail to recruit centromeric proteins, lag during embryonic divisions, and form micronuclei [52,53]. It is noteworthy that we also find lagging DNA and micronuclei in a fraction of dead *C. nouraguensis*/*C. becei* hybrid embryos, potentially indicating that paternal *C. becei* chromosomes fail to load centromeric proteins required for chromosome segregation.

Characteristics of incipient gynogenesis

Asexuality is rare in animals, suggesting that there are strong barriers that prevent its evolution from a sexual ancestor. However, it is largely unknown how the transition from sexuality to asexuality might occur, nor how the costs and benefits of such a transition might influence the longevity of a nascent asexual lineage. Some obligately gynogenetic species are composed entirely of females, and require that their eggs be fertilized and activated by males of a closely related species [11]. We hypothesize that the rare gynogenetic reproduction seen in *C. nouraguensis* x *C. becei* hybridizations could serve as a transitional state between sexual and obligate or facultative interspecies gynogenetic reproduction. Furthermore, we hypothesize that the diploid maternal inheritance observed in *C. nouraguensis* intraspecies crosses could be used as a stepping-stone towards either gynogenetic or parthenogenetic reproduction. However, the evolution of parthenogenesis from intraspecies *C. nouraguensis* crosses would also require that the oocyte not rely on sperm for centrioles and reactivation of the cell-cycle, and the evolution of gynogenesis from intraspecies crosses would require paternal genome loss. Nevertheless, both interspecies gynogenesis and intraspecies diploid maternal inheritance could be features of a nascent asexual lineage.

We have shown that diploid maternal inheritance in *C. nouraguensis* oocytes is the result of inheriting two homologous chromatids that have undergone meiotic recombination, and therefore fits a model of automixis in which two homologous chromatids are combined ("central fusion"). Because there is only a single recombination event that is biased towards the chromosome ends, inheriting two homologous chromatids either maintains heterozygosity across the entire chromosome or most of it (Fig 3B). However, recombination does occur in the middle of chromosomes at a lower frequency [32], which should eventually result in genome-wide homozygosity and inbreeding depression after many generations of automixis. Most *Caenorhabditis* species appear to be dioecious (females and males), with some exhibiting genetic hyperdiversity [54,55]. Therefore, inbreeding depression could be a sizable hurdle to overcome in the evolution of this form of gynogenesis from an obligately sexual *Caenorhabditis* ancestor.

Given that two copies of each maternal autosome are almost always inherited in the interspecies *C. nouraguensis* x *C. becei* cross, we were surprised to observe that some diploid fertile F1 are males. Indeed, sequencing data show that the three fertile males have only a single X chromosome (Fig S5 and Fig S7). Thus, missegregation of the X-chromosome during the modified female meiosis can result in only one X chromatid being inherited by the oocyte. Interestingly, two of the three fertile males were also aneuploid (triploid) for a single *C. nouraguensis* autosome, indicating that widespread chromosome missegregation occurred while producing these individuals. Generating males at a low frequency can theoretically aid the spread and maintenance of gynogenesis by transmitting alleles required for diploid maternal inheritance into neighboring sexual populations [56]. The production of males even at a low frequency can also help propagate an intraspecific gynogenetic lineage by enabling the activation of the egg and inheritance of centrioles without relying on males from a related species. This is observed in the nematode *Mesorhabditis belari,* in which only 9% of offspring are males and 91% are gynogenetically reproducing females [36]. Thus, it is notable that gynogenetic reproduction in *C. nouraguensis* x *C.*

becei hybridizations and *C. nouraguensis* intraspecies crosses already exhibits the ability to produce males.

In conclusion, our study establishes *C. nouraguensis* as a new genetic model system to study rare asexuality in animals. Further study of this system may provide insights into the mechanisms of diploid maternal inheritance and paternal genome loss, as well as the obstacles associated with a transition from sexual to asexual reproduction.

MATERIALS AND METHODS

Strain isolation and maintenance

All strains of *Caenorhabditis* used in this study were derived from single gravid females isolated from rotten fruit or flowers [57,58]. Strains of *C. nouraguensis* were kindly provided by Marie-Anne Félix ("JU" prefix) and Christian Braendle ("NIC" prefix). Most strains are outbred, except JU2079, QG2082 and QG2083, which are inbred lines derived from JU1825, QG704 and QG711, respectively. These inbred lines were used to generate the *C. nouraguensis* and *C. becei* genome assemblies. Strain stocks were stored at -80°. Strains were maintained at 25° on standard NGM plates spread with a thin lawn of *E. coli* OP50 bacteria [59].

Phylogenetic analysis

To construct a phylogeny, we used a subset of the coding sequences from Kiontke et al. [57]. The following genes were used: *ama-1, lin-44, par-6*, *pkc-3*, *W02B12.9*, *Y45G12B.2a*, *ZK686.3*, and *ZK795.3*. The *C. yunquensis* coding sequences were obtained from NCBI, while all other coding sequences were obtained from the caenorhabditis.org BLAST server (blast.caenorhabditis.org/#) using the *C. elegans* homolog as the query sequence. The coding sequences for each species were concatenated and aligned with MUSCLE [60] using default settings. A maximum likelihood phylogeny was made using PhyML 3.0 online (http://www/atgc-montpellier.fr/phyml/) [61] using a Generalized Time Reversible (GTR) substitution model with six substitution rate categories. Tree searching was performed using Nearest Neighbor Interchanges (NNIs). Branch support was determined by 100 bootstraps.

Quantifying strain viability

Strain viability was quantified as in [62]. Briefly, we crossed 10 virgin L4 females and males of the same strain on a single plate coated with palmitic acid. The plates were placed at 25°

overnight, allowing the worms to mature to adulthood and begin mating. The adult worms were then moved to a new plate rimmed with palmitic acid, allowed to mate and lay eggs for 1.5 hours at 25°, and then removed. The eggs laid within that time were immediately counted. Two days later, we placed the plates at 4° for 1 hr and counted the number of healthy L4 larvae and young adults per plate. We defined the percentage of viable progeny as the total number of L4 larvae and young adults divided by the total number of eggs laid.

DIC imaging of embryogenesis

Twenty-four hours after the L4 stage, we picked 20-40 gravid females into a 30 µl pool of 1x Egg Buffer (25 mM HEPES pH 7.4, 118 mM NaCl, 48 mM KCl, 2 mM EDTA, 0.5 mM EGTA) on a glass coverslip and dissected out embryos by cutting the adults in half using two needles like scissors. The embryos were then transferred with a glass capillary tube into a fresh pool of Egg Buffer to dilute any contaminating bacteria, and then placed onto a 2% agarose pad on a glass slide. The mounted embryos were put into a humid chamber for 20 minutes before adding a coverslip. The edges of the coverslips were sealed with petroleum jelly to prevent evaporation of the agarose pad. DIC z-stack images were captured every 3 minutes for 10 hours using a Nikon Eclipse 80i compound microscope (60x oil lens, 1.40 NA). Images were processed using Image J [63].

Calculating the frequency of rare interspecific F1

For each interspecies cross we set up 20-25 plates, each with one virgin L4 female crossed to a single virgin L4 male. The plates were placed at 25° overnight, allowing the worms to mature to adulthood and begin mating and laying eggs. To prevent overcrowding, the adult couples were moved to a new plate every day for three days. The number of eggs laid on each plate was

counted the day the parents were removed. Each plate was monitored for two days to check for the presence of rare viable F1, which were counted and moved onto a new plate.

Generating rare interspecific F1 and testing their fertility

To collect enough rare viable F1 animals for fertility testing and genotyping, we set up six cross plates, each with 30 *C. nouraguensis* L4 females and 30 *C. becei* L4 males and let them develop into adults overnight at 25°. We monitored the plates for the presence of viable F1 larvae each day for 5-6 days. Each viable F1 was moved to its own new palmitic acid-rimmed plate, and its fertility was tested as either an L4 or young adult by backcrossing it to one or two *C. nouraguensis* individuals of the opposite sex. F1 individuals were classified as sterile if they mated to *C. nouraguensis* but produced no F2 embryos, while F1 individuals were classified as fertile if they produced F2 embryos. Mating was inferred by the presence of a male-deposited copulatory plug on the female vulva [64]. After fertility testing and PCR genotyping, we found that hybrid males produced no embryos when crossed to *C. nouraguensis* females and were classified as sterile. However, they often failed to produce a copulatory plug, so we cannot tell whether sterility is due to abnormal germline development or defective mating.

To track the fate of the two maternal homologous chromosomes in subsequent crosses, we crossed two genetically distinct strains of *C. nouraguensis* (JU1825 and NIC59) to generate heterozygous *C. nouraguensis* NIC59/JU1825 females. Specifically, we crossed virgin L4 JU1825 females to NIC59 males and vice versa to generate female offspring that are heterozygous NIC59/JU1825 at all nuclear loci and carry either JU1825 or NIC59 mitochondria, respectively. We denote the genotype of these heterozygous females by the following nomenclature: “(mitochondrial genotype); nuclear genotype”. Therefore, the first cross produces *C. nouraguensis* (J); N/J females, while the second produces *C. nouraguensis* (N); N/J females (Table S1). We then crossed both types of *C. nouraguensis* N/J virgin females to *C. becei* QG711 males. We collected

the rare viable F1 from these interspecies crosses and tested their fertility by backcrossing them to the *C. nouraguensis* strain matching their mitochondrial genotype in order to avoid known cytoplasmic-nuclear incompatibilities within this species [62].

Generating worm and embryo lysates for PCR

Single worm PCR: Each adult worm was placed in a PCR tube with 10 µl of lysis buffer (1x Phusion HF buffer + 1.0% Proteinase K) and frozen at -80° for at least 15 minutes. The worms were then lysed by incubating the tubes at 60° for 60 mins and 95° for 15 mins. 1 µl of worm lysate was used in each 10 µl PCR reaction. Control lysates were generated by mixing 10-15 worms in lysis buffer.

Single embryo PCR: Dead embryos were picked into a 30 µl pool of 2 mg/ml chitinase on an 18x18 mm coverslip. OP50 bacteria were washed off embryos by pipetting the chitinase solution up and down. Using a glass capillary tube, embryos were transferred to a new pool of chitinase and washed again, and individual embryos were placed in a PCR tube with 5 µl of 2 mg/ml chitinase solution and incubated at room temperature for 2 hours. 5 µl of lysis buffer (2x Phusion HF Buffer + 2.0% Proteinase K) was added to each PCR tube and mixed by light vortexing. The samples were then frozen and lysed as in the single worm PCR protocol. 2.5 µl of embryo lysate was used in each 10 µl PCR reaction. Control lysates were generated by mixing 10-15 embryos in the same PCR tube.

PCR primers

Primer name	Sequence (5'-3')	Chromosome	Strains distinguished	Type of polymorphism
5.8S1	CTGCGTTACTTACCACGAATTGCAGAC	I (ITS2)	*C. n* vs *C. b*	PCR-RFLP (Hind-III)

KK-28S-22	CACTTTCAAGCAACCCGAC	I (ITS2)	*C. n* vs *C. b*	PCR-RFLP (Hind-III)
oPL20	CTGATGAGCATCGTCCGAC	II (W02B12.9)	*C. n* vs *C. b*	PCR-RFLP (EcoRI)
oPL21	CCTAGCTTGCAATCCACACG	II (W02B12.9)	*C. n* vs *C. b*	PCR-RFLP (EcoRI)
oPL78	TCCTCCAGCATATCCGCTCG	III	JU1825 vs NIC59	indel
oPL79	CAATTGCACGGAGAGACTGTTCATC	III	JU1825 vs NIC59	indel
oPL181	CGTCAAGATCAGATGCGAGACG	I	JU1825 vs NIC59	indel
oPL182	CAGTTGAGAACTGCCTGTCAGAC	I	JU1825 vs NIC59	indel
oPL318	GTGGCTTGTAGAGCTTGTGC	V	*C. n* vs *C. b*	indel
oPL319	GATCAATGATAGACATGGCC	V	*C. n* vs *C. b*	indel
oPL320	TGGTGTCGAATTCTCAAATTCC	X	*C. n* vs *C. b*	indel
oPL321	TAGGGGCAGAATATTGAACACTG	X	*C. n* vs *C. b*	indel
oPL356	TATTTGTGTGTTTGCCAGAGG	V	JU1825 vs NIC59	indel
oPL357	TCGAATACATTTGGCTTCACG	V	JU1825 vs NIC59	indel

The primers used in the PCR-RFLP polymorphism assays lie in conserved coding sequences that are easily amplified from a range of *Caenorhabditis* species [57]. Primers 5.8S1

and KK-28S-22 were originally used in Kiontke et al [57]. The primers used in the PCR indel polymorphism assays were generated after the assembly of the *C. nouraguensis* genome. Indel polymorphisms between NIC59 and JU1825 were found by manually screening *C. nouraguensis* (JU2079) scaffolds in IGV [65] for regions where JU1825 had read coverage but NIC59 did not (and vice versa). Indel polymorphisms between *C. nouraguensis* and *C. becei* were manually found by aligning homologous sequences on scaffolds assigned to a chromosome of interest.

Fixing and DAPI staining the female germline

Fixing and DAPI staining germlines was performed as in [66]. F1 L4 females were mated to *C. nouraguensis* L4 males. 24 hours later, we dissected the gonads from fertile F1 females and stained with DAPI. 30-40 females were picked into 15 µl of 1x Egg Buffer + 0.1% Tween-20 on a glass coverslip and their heads were cut off with needles to expel the gonad. After dissection, 15 µl of Fixation Solution (1x Egg Buffer + 7.4% formaldehyde) was added and mixed well by pipetting. Gonads were fixed for 5 minutes, then 15 µl of the mixture was removed and a Histobond slide was laid down gently on top of the coverslip. Excess liquid was removed with Whatman paper and samples were frozen by placing the slide on a metal block on dry ice for 10 minutes. Coverslips were then quickly flipped off with a razor blade and the slides were placed in a Coplin jar with -20° methanol for 1 minute. The slides were then moved to a Coplin jar with 1x PBS + 0.1% Tween-20 for 10 minutes, then a Coplin jar with 1x PBS + 0.1% Tween-20 + 5 µl of 5 mg/ml DAPI for 15 minutes, then a Coplin jar with 1x PBS + 0.1% Tween-20 for 20 minutes. Samples were then mounted with 11 µl Mounting Media (35 µl 2M Tris + 15 µl MilliQ dH_2O + 450 µl glycerol) and sealed with nail polish. Images were taken using a Nikon Eclipse 80i compound microscope and processed using Image J.

C. becei genome assembly and linkage map construction

The chromosomal reference assembly for *C. becei* is based on high-coverage paired-end and mate-pair short-read sequencing, low-coverage Pacific Biosciences long reads, and genetic linkage information from an experimental intercross family. We used two inbred lines, QG2082 and QG2083, derived from isofemale lines QG704 and QG711 respectively by sib-mating for 25 generations. QG704 and QG711 were isolated from independent samples of rotten flowers (QG704) or fruit (QG711) collected in Barro Colorado Island, Panama, in 2012 [58]. We generated conservative *de novo* assemblies for the inbred lines, identified SNPs that distinguish them, and then used a six-generation breeding design to generate recombinant populations (G_4BC_2) from which we generated a SNP-based linkage map. With the map-scaffolded conservative assembly, we were able to evaluate more contiguous, less conservative genome assemblies for consistency, and we selected one of these as our final *C. becei* genome. Each of these steps is described in detail below.

Sequencing

We extracted genomic DNA from QG2083 by proteinase K digestion and isopropanol precipitation [67] and prepared paired-end (PE) 600-bp insert and mate-pair (MP) 4-kb insert Illumina Nextera libraries, from which 100-bp reads were sequenced to approximately 30x and 60x expected coverage (see below) on an Illumina HiSeq 2000 at the NYU Center for Genomics and Systems Biology GenCore facility (New York, USA). PE reads for QG2082 were generated similarly, for 20x expected coverage. PE reads for G_4BC_2 mapping populations were generated from 250bp insert libraries sequenced to mean 4x coverage per line with 150-bp reads on a HiSeq 2500. FASTX Toolkit (v. 0.0.13; options '-n -l 25 -M 9 -Q 33'; http://hannonlab.cshl.edu/fastx_toolkit/) was used to trim low quality bases from PE reads, and NextClip (v. 1.3; [68]) was used to remove adaptors from MP reads and assess read orientation. Contaminating bacterial sequence was removed with Kraken (v. 1.0; [69]) using a database built

from NCBI nt (downloaded 10/06/2014), and sequencing errors were corrected with Blue (v. 1.1.2; [70]). Raw data is available from the NCBI SRA under project PRJNA525787.

Genome assembly for map construction

We assembled contigs and conservative scaffolds for QG2083 with the string graph assembler SGA [71]. Scaffolding required contigs to be linked by at least 5 unambiguously mapped mate-pair reads and full path consistency between contigs and all mapped mate-pair reads (option '--strict'). PacBio long reads (12x coverage, P4-C2 chemistry, Duke University Center for Genomic and Computational Biology) were used for a single round of gap closing and scaffolding with PBJelly (v. 13.10, minimum evidence of two reads; [72]), followed by scaffold breakage at any regions of mate-pair read discordance with REAPR (v. 1.0.17; [73]). This yielded a fragmented assembly of 9152 scaffolds of length at least 500 bp spanning 95.9 Mb, with half the assembly in scaffolds of 56 kb or more.

Variant calling

QG2082 reads were aligned to the QG2083 reference scaffolds with bwa mem (v. 0.5.9; [74]), processed with samtools (v. 1.2; http://www.htslib.org/) and Picard (v. 1.111; http://broadinstitute.github.io/picard/) utilities, and SNPs were called using the GATK HaplotypeCaller (v. 3.1-1; hard filtering on 'MQ < 40.0 || DP < 4 || FS > 60.0 || ReadPosRankSum < -8.0 || QD < 4.0 || DP > 80'; [75]). Fixed diallelic SNPs were supplemented with calls from reference mapping of the pooled G_4BC_2 data and, to mitigate potential mapping bias against highly divergent regions, SNP calls from whole genome alignment of a *de novo* assembly of G_4BC_2 data pooled with QG2083 data at 1:1 expected heterozygosity, using the heterozygous aware assembler Platanus [76] and Mummer [77]. This yielded a total of 1.63M diallelic SNPs across 6843 scaffolds spanning 89.2 Mb. These SNPs provide markers for genetic map construction.

Genetic map construction

We generated F_2 animals from reciprocal crosses between QG2083 and QG2082. We then performed 160 single-pair random-mating intercrosses among F_2s to generate G_3s, and again among G_3s to generate G_4s. These intercrosses allow additional meioses to expand the genetic map. We backcrossed G_4 females to QG2082 males, generating progeny carrying one recombinant version of the genome and one intact QG2082 genome. To increase the quantity of DNA representing these genomes, we crossed females to QG2082 males again and allowed the resulting G_4BC_2 populations to grow for a single generation before DNA extraction and library preparation. Data for 87 G_4BC_2 populations with at least 0.5x expected coverage were mapped to the QG2083 scaffolds and genotyped by HMM using a modified MSG pipeline (assuming six crossovers per assembled genome, genotyping error rates of 0.001, and a scaling parameter on transition probabilities of $1x10^{-11}$, taking the dominant parental assignment as a single genotype for each scaffold) [78]. Markers were filtered in r/qtl based on missing data (<50%) and segregation distortion (χ^2 test $p > 1x10^{-10}$), followed by removal of redundant markers [79]. Based on genotyping error rate estimates we further required a minimum of 70 SNP calls per scaffold and a minimum length of 1 kb, yielding 1337 non-redundant scaffold markers spanning 81.5 Mb. Six linkage groups were recovered over a wide range of minimum pairwise LOD scores, and within linkage group marker ordering was carried out by the minimum spanning tree method implemented in ASMap [80].

Assembly of the C. becei draft genome

Linkage group scaffolds were aligned against multiple Platanus *de novo* assemblies using the sequencing data from inbred lines and subsampling of the approximately 350x pooled data from G_4BC_2 lines, with the UCSC chain/net pipeline [81]. Genome evolution in the *Caenorhabditis*

genus occurs largely through intrachromosomal rearrangement, and 84-94% of the net for each *C. becei* linkage group aligned to the homologous *C. elegans* chromosome. The assembly most concordant with genetic data was selected, based on the number and aligned length of (1) scaffolds mapping to multiple linkage groups and (2) outliers in the ratio of genetic to physical distance. The selected assembly contained six cases where scaffolds mapped to multiple linkage groups – usually terminal regions of large scaffolds, with these terminal alignments spanning just over 1 Mb in total – and three scaffolds where mapping within linkage groups was inconsistent with the genetic data (median absolute deviation 99th percentile for the ratio of genetic to physical span), spanning 179 kb.

The draft assembly improved contiguity and incorporated several Mb of sequence not represented by the genetic map scaffolds, from 2483 redundant marker scaffolds to 256 final scaffolds spanning 84.9 Mb. We estimate a genome size of around 95 Mb based on mapped read-depth [71], with 90 Mb of that unique sequence amenable to assembly and variant calling.

C. nouraguensis genome assembly

The *C. nouraguensis* reference genome was generated from JU2079, an inbred strain derived from 28 generations of JU1825 sibling matings (Marie-Anne Félix, personal communication). Genomic DNA and RNA were purified from mixed-stage individuals and sent to Mark Blaxter at the University of Edinburgh for Illumina sequencing. 125-bp paired-end reads were generated from two libraries, one with inserts of ~400 bp (~55 million read-pairs), the other with inserts of ~550 bp (~54 million read-pairs) (SRA project accession PRJEB10884). After generating a preliminary assembly, we used BlobTools [82] for taxonomic classification. Some contigs matched *E. coli* (provided as food) and some matched an unsequenced bacterial species in the Firmicutes phylum. We extracted the Firmicutes contigs and used GSNAP [83] to remove matching read-pairs, and to remove any read-pairs matching the *E. coli* REL606 genome (Genbank

accession NC_012967), a strain closely related to OP50. We also removed reads failing Illumina's 'chastity filter' and used cutadapt to trim poor quality sequences (phred score < 10) and adapter sequences from the 3' ends of reads. We then performed error-correction using Musket [84] with a k-mer size of 28, and performed *de novo* genome assembly, scaffolding and gap closure using Platanus [76] with an initial k-mer size of 21. We then used REAPR [73] to break any misassembled scaffolds. The resulting assembly is approximately 73 Mb in size. We used BUSCO [85] to measure its completeness using a set of conserved genes, and find that our assembly contains 81.5% of conserved single-copy orthologs as a single copy, 9.8% as duplicates, and 3.6% as fragments, very similar to what is seen in the finished *C. elegans* genome assembly [85]. Using MUMMER [77], we ordered and oriented our *C. nouraguensis* scaffolds based on synteny to the *C. becei* genome assembly. Using this approach, some scaffolds remain unplaced and others may be misplaced, either because of true differences between the two species' genomes, or because MUMMER's alignments are noisy.

We also generated assemblies of the mitochondrial genomes of *C. becei* strain QG2083, and *C. nouraguensis* strain JU2079 using reads generated by Mark Blaxter's lab (EMBL ENA accession ERR1018617), filtered as above to remove *E. coli* reads, and down-sampled to 10 million read-pairs for *C. nouraguensis*. We then used the Assembly by Reduced Complexity (ARC) [86] pipeline to assemble mitochondrial genomes, using the *C. elegans* mitochondrial genome sequence as a starting point.

Whole-genome amplification and library preparation

After testing the fertility of rare viable offspring from crosses of *C. nouraguensis* JU1825/NIC59 females to *C. becei* males (see above), we prepared Illumina whole-genome sequencing libraries as follows. We first transferred each worm individually to a blank NGM plate with no OP50 lawn for 30 minutes to reduce the amount of contaminating bacterial DNA. We then

performed whole-genome amplification using the Qiagen REPLI-g Single Cell kit [87]. We picked individual worms into 4 µl of PBS sc and froze them at -20° for at least an hour. We thawed the samples and added 3 µl of Buffer D2, mixed well, and incubated at 65° for 20 minutes rather than the recommended 10 minutes to aid in worm lysis. The rest of the protocol was performed according to the manufacturer's guidelines. We purified the resulting amplified DNA using the Zymo Research Genomic DNA Clean & Concentrator kit (gDDC-10). We submitted approximately 0.5-0.8 ng of each sample to the Fred Hutchinson Cancer Research Center Genomics Core Facility. A uniquely barcoded sequencing library for each sample was made using the Illumina Nextera library prep kit and sequenced on an Illumina Hiseq2500 to generate 50-bp paired-end reads. We sequenced eleven fertile and ten sterile F1 individuals. We also sequenced a set of control samples so that we could determine how coverage varies across the genome for pure *C. nouraguensis* or *C. becei* populations, as well as to allow us to determine fixed SNPs between the NIC59 and JU1825 *C. nouraguensis* strains. Specifically, we sequenced genomic DNA derived from large populations of NIC59, JU1825 and QG711 (sample names: NIC59_bulk, JU1825_bulk and QG711_bulk). In order to determine whether SNP frequencies and coverage metrics behave as expected in heterozygous or hybrid triploid genomes, we sequenced three additional controls: (a) a single heterozygous NIC59/JU1825 female (sample name: F1_NIC59_JU1825); (b) a sample where we placed one NIC59 female and one JU1825 female in the same tube (sample name: NIC59plusJU1825); and (c) a sample where we placed one NIC59 female, one JU1825 female and one QG711 female in the same tube (sample name: NIC59plusJU1825plusQG711).

SNP calling, genotyping, and coverage calculations

Using GSNAP [83], we mapped the reads from each sample to a combined reference genome containing the *C. nouraguensis* and *C. becei* nuclear and mitochondrial genome assemblies, the *E. coli* REL606 genome sequence and the Firmicutes contigs described above.

We allowed GSNAP to report only a single map position for each read (--npaths=1). We further filtered read mappings, requiring mapq value of at least 20 to select uniquely mapping reads.

After preprocessing bam files by marking duplicates (using picard's MarkDuplicates, http://broadinstitute.github.io/picard/) and realigning indels (using GATK's RealignerTargetCreator and IndelRealigner tools [75]), we called SNPs in *C. nouraguensis* scaffolds using samtools mpileup [88] (ignoring indels, disabling the per-base alignment quality option and increasing the depth down-sampling parameter to 6660). We counted reads matching each allele using GATK's VariantAnnotator tool [75], disabling the down-sampling option and using the "ALLOW_N_CIGAR_READS" option. We noticed that the distribution of allele frequencies in our 'heterozygous' control samples was skewed towards the reference allele, likely because those reads are easier to map to the reference assembly. We therefore used this first round of SNP calls to remap all reads to the combined reference genome using GSNAPs "SNP-tolerant" mode that allows reads to map to either haplotype. SNPs were called a second time, after one additional level of read mapping filtering, where we used the R/Bioconductor Rsamtools package [89] to select only reads where the full length of the read could be aligned to the reference genome.

We then used the R/Bioconductor VariantAnnotation package [89] to select high-quality fixed differences between the NIC59 and JU1825 strains as follows: we required a SNP quality score of at least 100; that opposite alleles be fixed (non-reference frequencies of <5% and >95%) in the two strains; that read depth in some *C. nouraguensis* control samples be within typical range for that sample (5-50 for JU1825_bulk and NIC59_bulk, and 100-450 for the combined JU2079 samples); and that read depth be 0 in our *C. becei* control samples (QG711_bulk and the two QG2083 libraries). 337,493 SNPs passed these filters (an average of one SNP every 217 bp). To estimate mean allele frequencies in 50-kb windows across the genome, we counted the total number of reads matching NIC59 and JU1825 alleles across the window and divided the NIC59 count by the total count. We then used a circular binary segmentation algorithm, implemented in

the Bioconductor package DNAcopy [90], to estimate the locations of breaks between different haplotypes as well as the average allele frequency in each segment.

Using the same filtered bam files, we determined coverage at each base position using the samtools depth tool [88]. Examining coverage and aligned bases in our control samples (JU1825_bulk, NIC59_bulk and QG711_bulk) reveals very high within-species sequence diversity, as seen in some other nematodes [54,55,91]. This high diversity means that in some genomic regions, especially on the chromosome arms, short reads are unalignable to the reference genomes, resulting in many regions of no coverage. Other genomic regions show more aligned base-pairs, but still harbor many SNPs. Therefore, before calculating mean coverage metrics, we filtered the base positions under consideration to include only those that had coverage of at least 8 reads in the relevant control samples (JU1825_bulk and NIC59_bulk for the *C. nouraguensis* assembly and QG711_bulk for the *C. becei* assembly), and then determined mean values in 50-kb regions of each scaffold. This filtering mitigated diversity-related coverage variation a little, but even in control samples coverage is still lower on chromosome arms than centers. To generate per-chromosome copy number estimates (Fig. 4A), we manually defined 1-2 regions in the center of each chromosome that are well-covered in each of the control samples and took the mean of 50-kb window coverages in each region.

Fixing and staining embryos

60-80 gravid females were picked into 30 µl of 1x Egg Buffer + 0.1% Tween-20 on a glass coverslip and dissected in half with needles to release embryos. After the females were dissected, we waited for five minutes to allow the mostly 1-cell stage embryos to develop. A Histobond slide was then gently laid on top of the coverslip. Excess liquid was removed with Whatman paper and the samples were frozen by placing the slide on a metal block on dry ice for 10 minutes. Coverslips were then quickly flipped off with a razor blade and the slides were immediately placed in a Coplin

jar with -20° methanol for 10 min. The slides were then moved to a Coplin jar with -20° acetone for 10 min. The slides were washed three times for 10 mins each in Coplin jars with 1x PBS + 0.1% Tween-20, then blocked for 30 mins in a Coplin jar with 1x PBS + 0.1% Tween-20 + 0.5% BSA + 0.02% sodium azide (blocking buffer). Each slide was then incubated overnight at 4° with a 1:100 dilution of both mouse monoclonal anti-α-tubulin (clone DM1A, Sigma) and rabbit polyclonal anti-γ-tubulin (ab50721, abcam) primary antibodies in blocking buffer. The next day, the slides were washed three times for 10 mins each in Coplin jars with 1x PBS + 0.1% Tween-20. Each slide was then incubated in the dark for 2 hours at room temperature with a 1:1000 dilution of both Alexa-Fluor 488 goat anti-mouse and Rhodamine Affinipure goat anti-rabbit secondary antibodies (Jackson ImmunoResearch) diluted in 1x PBS + 0.1% Tween-20. The slides were moved to a Coplin jar with 1x PBS + 0.1% Tween-20 for 10 minutes, then a Coplin jar with 1x PBS + 0.1% Tween-20 + 5 µl of 5 mg/ml DAPI for 15 minutes, then a Coplin jar with 1x PBS + 0.1% Tween-20 for 20 minutes. Samples were mounted with 12 µl VectaShield (H-1000, Vector Laboratories) and sealed with nail polish. Samples were imaged using a Nikon Eclipse 80i compound microscope with a 100x oil objective (1.45 NA). Images were processed using Image J.

We only analyzed embryos at early stages of embryogenesis (1-4 cell stage). In normal embryos at this stage, the DNA in the two polar bodies appears as two distinct clumps at the periphery of the embryo that are easily distinguishable from other embryonic nuclei. Polar bodies in hybrid embryos were considered to have abnormal morphologies if they were unlike those observed in the JU1825 control. This encompasses a range of abnormalities such as not being round, being larger, or having easily distinguishable chromatids.

Male UV irradiation

Virgin *C. nouraguensis* L4 males and L4 females were collected and separately placed onto two new NGM plates seeded with OP50 and rimmed with palmitic acid. We added a few females to

the male plate to coax the males to stay on the surface of the plate. The next day, now young adult males were picked onto a blank NGM plate rimmed with palmitic acid. This plate was placed in a CL-1000 UV Crosslinker (Ultra-Violet Products) without a lid and the males were exposed to 70,000 μJ/cm^2 254-nm UV radiation. Immediately afterward, the males were picked onto new NGM plates seeded with OP50 and rimmed with palmitic acid. Each plate had 30-90 irradiated males and 30-90 young adult virgin females. The next day, rare viable larvae were picked from the cross plates onto a new NGM plate seeded with OP50 and rimmed with palmitic acid. When these progeny reached adulthood, they were individually frozen, lysed and PCR genotyped.

We tested the following UV exposures: 15,000, 40,000, 50,000, 60,000, 70,000, 80,000, 150,000 and 250,000 μJ/cm^2. Males treated with lower exposures (15,000 and 40,000 μJ/cm^2) were able to produce many viable progeny, indicating that their sperm DNA was not damaged enough to induce paternal genome loss. Males treated with the highest exposures (150,000 and 250,000 μJ/cm^2) mostly stopped moving and never recovered. We found that males treated with 70,000 μJ/cm^2 were healthy enough to mate and produce many dead fertilized embryos, but relatively few viable progeny.

Each 30 female x 30 male or 90 female x 90 male plate eventually became overcrowded with dead embryos, making it difficult to manually quantify their exact number. Instead of counting each embryo on these plates, we performed a five female x five male cross in parallel and counted their dead embryos. We then determined the average number of dead embryos per female on the 5 female x 5 male plates and multiplied that by the number of total females to get a rough estimate of the total number of dead embryos.

ACKNOWLEDGMENTS

We thank Marie-Anne Félix and Christian Braendle for providing the strains of *C. nouraguensis* used in this study; Max Bernstein, Vicky Cattani, Taniya Kaur, Jasmine Nicodemus

and Annalise Paaby for help performing *C. becei* mapping crosses and preparing sequencing libraries; Mark Blaxter, Lewis Stevens and members of the *Caenorhabditis* Genomes Project for sequencing *C. nouraguensis* (JU2079) as well as providing a public BLAST server of newly sequenced *Caenorhabditis* species (http://blast.caenorhabditis.org/); Maulik Patel for help in preparing DNA for *C. nouraguensis* genome sequencing (JU1825 and NIC59); Lews Caro and Sam Hart for additional experiments; Jihong Bai for sharing his UV-irradiator; Lamia Wahba for advice on single-worm sequencing; Needhi Bhalla and Mara Schvarzstein for discussions of *C. elegans* female meiosis; Jim Priess for discussions of *C. elegans* development; and Hannah Seidel for advice on time-lapse imaging of *Caenorhabditis* embryos. We also thank Barbara Wakimoto, Diane Shakes, Lisa Kursel, Irini Topalidou, Ofer Rog and members of his lab, and members of the Ailion lab for comments on the manuscript. We thank the Fred Hutchinson Genomics core for Illumina library preparation and sequencing. P.L. was supported in part by a National Institutes of Health Institutional Training Grant (Public Health Service, National Research Service Award, T32GM007270 from National Institute of General Medical Sciences). This work was supported by the NYU CGSB Genomics Core facility and NYU IT High Performance Computing resources, NIH grant R01 GM121828 to M.V.R, NIH grant R01 GM074108 to H.S.M, and an NSF CAREER Award (MCB-1552101) to M.A.

AUTHOR CONTRIBUTIONS

P.L. performed the majority of the experiments and analyzed the data. J.M.Y. made the *C. nouraguensis* genome assembly, analyzed the single-worm genome sequencing data, and wrote the associated methods section. L.M.N. and M.V.R. constructed the genetic map and genome assembly of *C. becei* and wrote the corresponding methods section. A.I. and M.P. helped perform crosses and PCR assays to classify rare viable F1. H.S.M. and M.A. provided funding and

supervised the project. P.L. wrote the original draft of the manuscript. The final draft was written by P.L., J.Y.M., H.S.M. and M.A., with input and edits from L.M.N. and M.V.R.

DECLARATION OF INTERESTS

The authors declare no competing interests.

FIGURE CAPTIONS

Fig 1. Crossing *C. nouraguensis* females to *C. becei* males results in sterile F1 with hybrid genotypes and fertile F1 with only-maternal genotypes. (A) A maximum likelihood phylogeny of several *Caenorhabditis* species closely related to *C. nouraguensis* and *C. becei*, with strain names in parentheses. *C. elegans and C. remanei* were used as outgroups. The scale bar represents 0.10 substitutions per site. Bootstrap support values are indicated to the left of each node (percent of 100 bootstrap replicates). See Stevens et al. (2019) for a more complete *Caenorhabditis* phylogeny [58]. **(B)** Frequency of viable F1 adults in crosses between *C. nouraguensis* and *C. becei*. NIC54 females yield a significantly higher proportion of viable F1 adults when crossed to *C. becei* (QG711) males than either JU1825 or NIC59 females (Chi-square with Yates correction, P=0.0065 NIC54 vs. JU1825, P=0.0005 NIC54 vs. NIC59). There was not a significant difference in the frequency of rare viable F1 adults produced by JU1825 and NIC59 females (Chi-square with Yates correction, P=0.49). The crosses between *C. becei* females and *C. nouraguensis* males serve as controls for accidental contamination of plates with embryos or larvae from either parental species -- no viable adults were found among more than 12,000 F1 screened for each cross (Fig S2). **(C)** Flowchart showing how fertility of rare viable F1 was tested (also see Materials and Methods). The gel shows how a PCR-RFLP assay distinguishes between *C. nouraguensis* and *C. becei* alleles at the ITS2 locus. **(D)** Tables showing the relationship between the fertility, genotype, and sex of rare viable F1 derived from crossing either *C. nouraguensis* (JU1825) females to *C.*

becei (QG711) males (top table, genotyped at the W02B12.9 locus) or *C. nouraguensis* (NIC54) females to *C. becei* (QG711) males (bottom table, genotyped at the ITS2 locus). Both sterile and fertile F1 exhibited a more strongly female-biased sex ratio than that seen in intraspecies crosses (Fig S1).

Fig 2. Fertile interspecific F1 females are diploid. **(A)** Schematic of one of the two germlines of a *Caenorhabditis* female. The germline is a syncytial tube with nuclei (depicted as small circles) hugging its circumference. Germline nuclei are generated from mitotically dividing stem cells at the distal tip and migrate proximally while undergoing meiotic prophase. Homologs of each of the six chromosomes replicate their DNA, with the resulting sister chromatids held together by sister chromatid cohesion (purple lines). Homologous chromosomes undergo one crossover biased towards a chromosome end and are remodeled into a cruciform structure. Eventually, cell membranes form around the nuclei, resulting in mature oocytes. In mature oocytes, homologous chromosomes and their sister chromatids form bivalents that are held together by a combination of sister chromatid cohesion and recombination. The -1 oocyte is fertilized by sperm, triggering the reductional first meiotic division in which sister chromatid cohesion is lost between homologs, allowing them to segregate during anaphase I. One set of homologs is segregated into the first polar body. During the second meiotic division, sister chromatid cohesion is lost between sister chromatids, which then segregate during anaphase II. One chromatid is segregated into the second polar body and the other is inherited by the oocyte. **(B)** Because only one crossover occurs per homologous set of chromosomes, diploid individuals have six bivalents (6 DAPI-staining bodies) while triploids have six bivalents and six univalents (12 DAPI-staining bodies). **(C)** Most *C. nouraguensis* (JU1825), *C. becei* (QG711) and fertile F1 females have 6 DAPI-staining bodies, consistent with being diploid for six chromosomes. However, some fertile F1 females have a

slightly higher number of DAPI-staining bodies, suggesting they are mostly diploid, but inherit some extra pieces of DNA. See Fig S4 for examples of DAPI staining.

Fig 3. Fertile interspecific F1 inherit two randomly selected homologous chromatids from each maternal bivalent. (A) Schematic of how we determined which two chromatids are inherited from each maternal *C. nouraguensis* bivalent. Two genetically distinct strains of *C. nouraguensis*, NIC59 and JU1825, were crossed to make heterozygous NIC59/JU1825 females, which were then crossed to *C. becei* (QG711) males. Viable F1 progeny were collected, assayed for fertility by backcrossing, and prepared for whole-genome amplification and sequencing. **(B)** The six possible ways to inherit two chromatids from a bivalent. Four have distinct chromosomal genotypes (Sisters_1, Sisters_2, Homologs_1 and Homologs_2), and two have genotypes that cannot be distinguished in our short-read sequencing data because they both result in heterozygosity across the entire chromosome (Homologs_3). **(C)** An example of whole-genome genotyping data from a single fertile F1 female (F1_5). Each plot represents one of the six chromosomes. Each point represents the average NIC59 SNP frequency in 50-kb windows ordered along the chromosome; haplotype change points and average allele frequency for each segment are shown by the green horizontal lines. The reference assembly is fragmented into scaffolds that we ordered and oriented on chromosomes using synteny; gray vertical lines represent breaks between scaffolds. The combination of two chromatids that best matches the genotyping data is shown underneath each plot. Genotyping and coverage plots for all F1 are shown in Figs S5 and S7. One fertile F1 gave ambiguous genotypes and was excluded from further analysis (F1_25); this individual had a particularly high percentage of contaminating bacterial reads and low coverage of the *C. nouraguensis* genome (Table S1). **(D)** Frequency of the five distinguishable chromosome genotypes when combining all fertile F1 genotyping data. The table also shows the expected frequency of the five genotypes if any two chromatids were randomly inherited and if any two

homologous chromatids were inherited. The frequencies observed in the fertile F1 are not different from those expected from random inheritance of two homologous chromatids (Fisher's exact test, P=0.41). Hemizygous X chromosomes in males and triploid autosomes were excluded from the analysis.

Fig 4. Sterile interspecific F1 inherit a diploid *C. nouraguensis* genome and a haploid *C. becei* genome. (A) The normalized read coverage for all autosomes in eight sterile F1 with a clear genotype. Coverage is normalized to the *C. nouraguensis* chromosome I coverage in each individual, which is set to two. Schematics below the graph show sterile F1 that are fully triploid hybrids (all cells of an F1 embryo have a diploid *C. nouraguensis* genome and a haploid *C. becei* genome) or diploid-triploid mosaic hybrids (all cells of an F1 embryo have a diploid *C. nouraguensis* genome, but only a subset of cells inherit the haploid *C. becei* genome). **(B)** An example of whole-genome *C. nouraguensis* genotyping data from a single sterile F1 male (F1_17). Each plot represents one of the six chromosomes. Each point represents the average NIC59 SNP frequency (after removing *C. becei* reads) in 50-kb windows along the physical length of the chromosome; haplotype change points and average allele frequency for each segment are shown by the green horizontal lines. The gray vertical lines represent breaks between scaffolds. The combination of two *C. nouraguensis* chromatids that best matches the genotyping data is shown underneath each plot. Genotyping and plots for all sterile F1 are shown in Figs S5 and S7. We excluded two sterile F1 from further analysis because they gave ambiguous genotypes (F1_18 and F1_26). **(C)** Frequency of the five distinguishable *C. nouraguensis* chromosome genotypes when combining all sterile F1 genotyping data. The table also shows the expected frequency of the five genotypes if any two chromatids were randomly inherited and if any two homologous chromatids were inherited. The frequencies observed in the sterile F1 are not different from those expected from random inheritance of two homologous chromatids (Fisher's exact test, P=0.78). **(D)**

Frequency of *C. nouraguensis* chromosome genotypes when combining all fertile and sterile F1 genotyping data. The frequencies observed are not different from those expected from random inheritance of two homologous chromatids (Fisher's exact test, P=0.85).

Fig 5. Dead interspecific F1 embryos inherit the *C. becei* X-chromosome and two maternal homologous chromatids. (A) Schematic illustrating how dead F1 embryos and viable F1 progeny were generated for PCR genotyping experiments. **(B)** An example of a DNA gel showing the chromosome X genotypes (oPL320+321) of rare viable F1 adults (top gel) and dead F1 embryos (bottom gel). The graph shows that no viable F1 animals inherited the *C. becei* X-chromosome, but half of the dead embryos inherited it. **(C)** An example of a DNA gel showing the chromosome V genotypes (oPL318+319) of dead F1 embryos. The graph shows that most dead F1 embryos inherited chromosome V from both parents but that some inherited only a maternal (*C. nouraguensis*) copy. **(D)** An example of a DNA gel showing the chromosome I genotypes (oPL181+182) of dead F1 embryos. Importantly, the primers used in this PCR reaction do not produce products when using a control *C. becei* QG711 embryo lysate as template, so any signal should be from *C. nouraguensis* templates. The graph shows that almost all dead F1 embryos have a heterozygous NIC59/JU1825 genotype. **(E)** A one-cell stage embryo derived from crossing *C. nouraguensis* (NIC59) females to *C. nouraguensis* (NIC59) males, fixed and stained for DNA (cyan), γ-tubulin (magenta), and α-tubulin (yellow). γ and α-tubulin staining shows the mitotic spindle, which helps determine how many cells there are in the embryo and at what point those cells are in the cell cycle. The white lines outline cells. The two polar bodies that remain associated with the embryo are indicated by arrowheads. **(F)** An intraspecies *C. nouraguensis* embryo with only one polar body. **(G)** A hybrid embryo with only one polar body, derived from crossing *C. nouraguensis* (NIC59) females to *C. becei* (QG711) males. **(H)** A hybrid embryo with zero polar bodies. Scale bars (E-H): 20 μm. **(I)** Roughly half the hybrid embryos have only one polar body. By

contrast, embryos derived from *C. nouraguensis* intraspecies crosses almost always have two polar bodies. “Two abnormal” refers to embryos that have two polar bodies, but one or both have an abnormal structure. “One abnormal” refers to embryos that have a single polar body with an abnormal structure.

Fig 6. Cytological characterization of early embryonic development in interspecies hybrids. **(A-H)** A set of fixed embryos that summarize early embryonic development in *C. nouraguensis* intraspecies crosses (NIC59 female x NIC59 male). Embryos stained for DNA (cyan), α-tubulin (yellow) and γ-tubulin (magenta). Scale bars: 20 μm. **(A)** When the sperm fertilizes the oocyte, it deposits a condensed haploid paternal genome (“p”) and centrioles into the egg. The centrioles gather γ-tubulin, which nucleates microtubule polymerization (two magenta dots). Fertilization triggers the female meiotic divisions, resulting in two polar bodies (“pb”) and the formation of a haploid maternal pronucleus (“m”). **(B)** The two pronuclei decondense and migrate towards each other. Centrosomes remain associated with the paternal pronucleus. **(C)** The two pronuclei meet. **(D)** Maternal and paternal chromosomes align along the metaphase plate of the first mitotic spindle. **(E)** Sister chromatids segregate to opposite spindle poles during anaphase and **(F)** form interphase nuclei after cytokinesis. **(G)** A two-cell embryo with both cells undergoing anaphase. **(H)** A four-cell stage embryo with all cells in interphase. **(I-L)** Hybrid embryos derived from *C. nouraguensis* (NIC59) female x *C. becei* (QG711) crosses. **(I)** Centrosomes in hybrid embryos can be dissociated from the male pronucleus during pronuclear migration. Both pronuclei are condensed. **(J)** A one-cell hybrid embryo with misaligned DNA at metaphase (arrowhead). **(K)** A two-cell hybrid embryo with lagging DNA between the two interphase cells (arrowhead). **(L)** A two-cell hybrid embryo during interphase. One cell has an extra smaller nucleus (micronucleus, arrowhead). **(M)** Quantification of embryos with abnormalities like those shown in Fig 6 I-L.

Fig 7. Diploid maternal inheritance can occur independently of interspecies hybridization. **(A)** Flowchart illustrating how the UV irradiation experiments were conducted. **(B)** A DNA gel showing the chromosome I genotypes (oPL181+182) of several rare viable F1 derived from crossing either *C. nouraguensis* JU1825 females to UV-irradiated *C. nouraguensis* NIC59 males (J♀ x N♂ UV) or NIC59 females to UV-irradiated JU1825 males (N♀ x J♂ UV). The sex of the rare viable F1 is depicted above each lane, with an identifying number as subscript. **(C)** A DNA gel showing the chromosome III and V genotypes (oPL78+79 and oPL356+357) of the rare F1 from Fig 7B that had a maternal genotype for chromosome I. All also had a maternal genotype at these two markers. **(D)** A table quantifying the frequency of gynogenetically-produced offspring from all *C. nouraguensis* intraspecies UV experiments (two for each cross). **(E)** A table quantifying the number of DAPI staining bodies in the -1 oocytes of gynogenetically-produced females from *C. nouraguensis* intraspecies UV experiments. **(F)** A two-cell embryo derived from an intraspecies *C. nouraguensis* cross (JU1825♀ x NIC59♂). Two polar bodies are indicated by white arrowheads. White lines outline cells. Scale bar: 20 μm. **(G)** A two-cell embryo derived from an intraspecies *C. nouraguensis* cross with irradiated males (JU1825♀ x NIC59♂ UV). Two polar bodies are indicated by white arrowheads. Lagging DNA (likely UV-irradiated paternal DNA) is indicated by the white arrow. **(H)** Quantification of polar bodies in *C. nouraguensis* intraspecies crosses.

Fig 8. Model for diploid maternal inheritance in *C. nouraguensis* oocytes. (A) Schematic of canonical meiotic divisions in *C. elegans*. Upon fertilization, each maternal bivalent (only one shown here) randomly bi-orients its homologs on the meiotic spindle, cohesion is lost between homologous chromosomes and homologs segregate. One set of homologs segregates into the first polar body while the other is retained in the oocyte (Anaphase I and Cytokinesis). Then the half-bivalent in the oocyte randomly bi-orients on the meiotic spindle, sister chromatid cohesion is lost and sister chromatids segregate. One sister chromatid is segregated into the second polar body

while the other is retained in the oocyte (Anaphase II and Cytokinesis). Thus, the oocyte inherits only one random chromatid from each bivalent. **(B)** One model for how female meiosis could be modified to inherit two random homologous chromatids from a bivalent. Upon fertilization, the bivalent randomly bi-orients its homologs on the meiotic spindle and cohesion is lost between homologous chromosomes as is normal. Homologs segregate but cytokinesis fails (Anaphase I) and both half-bivalents remain in the oocyte. Each half-bivalent then bi-orients on the meiotic spindle, sister chromatid cohesion is lost, and sister chromatids segregate. One chromatid from each half-bivalent segregates into the second polar body while the other is retained in the oocyte (Anaphase II and Cytokinesis). Thus, the oocyte inherits two random homologous chromatids from a bivalent.

SUPPLEMENTAL FIGURE CAPTIONS

Fig S1. Control crosses to measure intra-strain viability. Wild isolates of *C. becei* (QG704 and QG711) and *C. nouraguensis* (NIC59 and JU1825) have high levels of intra-strain viability. All strains have a sex ratio skewed towards females, some of which are statistically significant (Fisher's exact test with Bonferroni correction, JU1825 p=1.0, NIC59 p=0.06, QG711 p=0.03, QG704 p=0.03).

Fig S2. Summary of interspecies crosses. Rows show the females of each cross and males are shown in columns. The wild isolate strains used for each species are indicated. Black boxes are intraspecies crosses. Grey boxes are untested interspecies hybridizations. Rare viable F1 adults are present only when crossing *C. nouraguensis* females to *C. becei* males. Rare viable but sick F1 larvae are present in both directions of *C. becei* x *C. yunquensis* crosses. Worms mate but do not produce F1 embryos in *C. panamensis* female x *C. nouraguensis* male and *C. becei* female x

C. panamensis male crosses. At least 12,000 dead F1 were screened for each cross that gave embryos.

Fig S3. Fertile progeny with a maternal genotype and sterile progeny with a hybrid genotype are produced when *C. nouraguensis* females are crossed to males of a different *C. becei strain*. (A) We tested the fertility of rare viable F1 derived from *C. nouraguensis* JU1825 x *C. becei* QG704 crosses by backcrossing to JU1825 individuals of the opposite sex. F1 were then genotyped at the ITS2 locus using a PCR-RFLP assay. **(B)** A gel showing the sex, fertility and genotype at the ITS2 locus of viable adult F1. All fertile F1 have a maternal genotype, with one exception: one hybrid F1 female laid inviable F2 embryos (F*, still considered fertile). All sterile F1 had a hybrid genotype. **(C)** A table summarizing the genotyping data in (B).

Fig S4. Fertile F1 females are diploid. The -1 oocytes from *C. nouraguensis* JU1825 and *C. becei* females primarily have six DAPI- staining bodies (two examples shown here). Most fertile F1 females derived from JU1825 female x QG711 male crosses have six DAPI-staining bodies (Example fertile F1 female #1). A minority have eight DAPI-staining bodies. In three of these cases, there appear to be seven relatively normal sized DAPI bodies plus a very small one (Example fertile F1 female #2, small DAPI body highlighted by white arrowhead). In the other two cases, all eight DAPI bodies appear roughly equal in size (Example fertile F1 female #3). This higher number of DAPI-staining bodies is not the chance observation of a low frequency meiotic defect in a nucleus that happens to be in the -1 oocyte position (for example, homologs fail to recombine and increase the number of univalents) because we observed the same number of DAPI-staining bodies in both germlines of the same fertile F1 female. We hypothesize that these extra DAPI-staining bodies represent extra DNA (either maternal or paternal) in addition to the two chromatids inherited from each maternal bivalent. Scale bar: 5 μm.

Fig S5. Fertile F1 inherit two randomly selected homologous chromatids from each maternal bivalent. (A) The six possible ways of combining two of the four genetically distinct chromosomes in a bivalent are illustrated, with their expected genotypic signature below them. There are five distinct genotypic signatures. Two result from combining sister-chromatids and are called "Sisters_1" and "Sisters_2". Three result from combining homologous chromosomes and are called "Homologs_1", "Homologs_2" and "Homologs_3". (**B)** A table summarizing the genotype of each maternal chromosome for each sequenced F1 individual. The F1's sex and fertility are noted. Each individual's ploidy is inferred from the genotyping data. The genotype "Homologs_ambiguous" refers to chromosomes that are heterozygous in their centers, but one end of the chromosome is not obviously heterozygous (N/J) or homozygous for either NIC59 or JU1825. The genotype "Hemizygous X" refers to hemizygous X-chromosomes in males that have half the read depth of the autosomes. The genotype "Triploid" refers to chromosomes that have three copies instead of two based on relative read depth and whole-chromosome genotype. The "Sisters_3" genotype refers to chromosomes that have inherited two non-recombinant JU1825 chromatids. Three fertile females (F1_8, F1_11 and F1_39) have NIC59 and JU1825 alleles in the center of their chromosomes, but exhibit a slight skew from the expected 0.50 NIC59 allele frequency (Fig S7). We hypothesize that this skew is due to contaminating DNA derived from backcrossing each female when testing her fertility. For example, a viable female that was backcrossed to a JU1825 male would carry JU1825 sperm and therefore JU1825 DNA in her spermatheca. In this case, the contaminating DNA would skew the female's entire genome to a lower NIC59 SNP frequency. Consistent with this, in all three females the more abundant allele matches the genotype of the male she was backcrossed to (Table S1). Correcting for this potential backcrossing contamination, the genotypes of all the chromosomes in these three females are consistent with the inheritance of two homologous chromatids. One fertile female (F1_25) and two

sterile females (F1_18 and F1_26) have a very low proportion of NIC59 reads across their entire genome (Fig S7). We hypothesize this skew is due to contaminating DNA from JU1825 males during fertility testing and poor lysis of the female (Table S1). The low proportion of NIC59 reads made it difficult to infer actual maternal chromosome genotypes and are therefore categorized as "ambiguous". **(C)** Tables summarizing the frequency of genotypes per chromosome in all fertile F1, all sterile F1, or a combination of all fertile and sterile F1.

Fig S6. Genotypic signatures of multiple potential mechanisms of diploid maternal inheritance. (A) A schematic of the cross used to determine how diploidy is restored in gynogenetically produced offspring in the interspecies cross. Heterozygous (NIC59/JU1825) *C. nouraguensis* females are crossed to *C. becei* (QG711) males. Individual viable offspring resulting from the hybridization undergo whole genome sequencing. **(B)** If diploid maternal inheritance results from mitotic (apomixis) rather than meiotic divisions, then viable F1 are clones of their mother and will be heterozygous NIC59/JU1825 across their entire genome (0.5 NIC59 allele frequency). **(C)** Diploid maternal inheritance can occur through endomitosis, which is when a haploid maternal genome replicates without a cell division. This results in two exact copies of each chromosome and therefore homozygosity for either NIC59 (1.0 NIC59 allele frequency) or JU1825 alleles (0.0 NIC59 allele frequency) across the entire genome. **(D)** Diploid maternal inheritance can occur through automixis (combining two of the four meiotic products). Combining two homologous chromatids will result in heterozygosity in the center of a chromosome, and heterozygosity or homozygosity at the chromosome ends. Combining two sister chromatids will result in homozygosity in the center of a chromosome and heterozygosity at one of the ends.
Inheriting two sister chromatids for one chromosome and two homologous chromatids for another chromosome in the same genome is theoretically possible, but not depicted here.

Fig S7. Fertile F1 inherit two randomly selected homologous chromatids from each maternal bivalent. Each of the following pages contains plots describing whole-genome sequencing data of either a rare viable F1 individual or a control DNA sample. The sample name is at the top of each page, along with the individual's sex, fertility and strain it was backcrossed to for fertility testing (if applicable). Each page has five rows of plots. The first row shows the genotypes of the sample's *C. nouraguensis* maternal chromosomes (i.e. average NIC59 allele frequency in 50-kb windows across the *C. nouraguensis* assembly). Haplotype change points and average allele frequency for each segment are shown by the green horizontal lines. The second and third rows show the sample's average read coverage of the *C. becei* and *C. nouraguensis* assemblies in 50-kb windows. The fourth and fifth rows show the average GC content of the *C. becei* and *C. nouraguensis* assemblies in 50-kb windows. The gray vertical lines represent breaks between scaffolds.

Fig S8. Fertilization with UV-irradiated sperm does not cause frequent diploid maternal inheritance in intraspecies crosses. (A) Fertilization with UV-irradiated sperm does not significantly increase diploid maternal inheritance in *C. nouraguensis* intraspecies crosses. Heterozygous *C. nouraguensis* (NIC59/JU1825) females were mated to UV-irradiated *C. nouraguensis* (NIC59) males. Dead embryos produced by this cross were PCR genotyped at a single autosomal locus (oPL78+79). The gel shows the genotypes of a fraction of the dead embryos assayed. Most embryos had either a JU1825 (11/31) or NIC59 genotype (17/31), consistent with haploid maternal inheritance and destruction of the paternal NIC59 genome. Although 3/31 embryos had a heterozygous genotype (red stars), we found that UV-irradiation can fail to completely destroy the paternal genome (see Fig S8B), suggesting that these three heterozygotes may result from haploid maternal inheritance of a JU1825 allele and haploid paternal inheritance of a NIC59 allele due to incomplete destruction of paternal DNA. **(B)** The

paternal genome is not always eliminated by UV irradiation. *C. nouraguensis* (JU1825) females were mated to UV-irradiated *C. nouraguensis* (NIC59) males. Dead embryos produced by this cross were PCR genotyped at a single autosomal locus (oPL78+79). The gel shows the genotypes of a fraction of the dead embryos assayed. Red stars indicate cases in which the UV-irradiated paternal NIC59 DNA can be detected.

Video S1. *C. nouraguensis* (JU1825) embryonic development. DIC time-lapse imaging of embryos derived from JU1825 female x JU1825 male crosses. Most develop into larvae, but two embryos fail to develop. Dissection and mounting of embryos causes some embryos to arrest at approximately the one-cell stage.

Video S2. *C. becei* (QG711) embryonic development. DIC time-lapse imaging of embryos derived from QG711 female x QG711 male crosses**.** Most develop into larvae, but one embryo fails to develop. Dissection and mounting of embryos causes some embryos to arrest at approximately the one-cell stage.

Video S3. *C. becei* female x *C. nouraguensis* male embryonic death. DIC time-lapse imaging of embryos derived from *C. becei* QG711 female x *C. nouraguensis* JU1825 male crosses**.** These embryos undergo cell divisions until approximately the 32-cell stage at which point they stereotypically arrest and fail to undergo further divisions. The embryos come out of focus at the end of the video.

Video S4. *C. nouraguensis* female x *C. becei* male embryonic death. DIC time-lapse imaging of embryos derived from *C. nouraguensis* JU1825 female x *C. becei* QG711 male crosses. These embryos arrest either at early or later stages of development. The early-arresting embryos

generally have abnormal cell membrane morphologies. Specifically, some arrested embryos have faint cell membranes that appear to distend and take up more space than the normally more rounded cells seen in the early embryos of either parental species. Also, some early-arresting embryos have many nuclei but no discernible cell membranes separating them. The embryos that arrest at later stages have superficially normal cell and nuclear morphologies and undergo cell divisions until approximately the 44-87 cell stage. After this point, the cells in these embryos largely halt their divisions, with many appearing to be dissociated from one another, rounded, and of variable size. One common feature of the early and late-arresting embryos is that both can have multinucleate cells.

REFERENCES

1. Green RF, Noakes DLG. Is a little bit of sex as good as a lot? J Theor Biol. 1995;174: 87–96. doi:10.1006/jtbi.1995.0081
2. D'Souza TG, Michiels NK. The costs and benefits of occasional sex: Theoretical predictions and a case study. J Hered. 2010;101: 34–41. doi:10.1093/jhered/esq005
3. Stelzer C-P, Lehtonen J. Diapause and maintenance of facultative sexual reproductive strategies. Philos Trans R Soc B Biol Sci. 2016;371: 20150536. doi:10.1098/rstb.2015.0536
4. Burke NW, Bonduriansky R. Sexual Conflict, Facultative Asexuality, and the True Paradox of Sex. Trends in Ecology and Evolution. Elsevier Ltd; 2017. pp. 646–652. doi:10.1016/j.tree.2017.06.002
5. Gibson AK, Delph LF, Lively CM. The two-fold cost of sex: Experimental evidence from a natural system. Evol Lett. 2017;1: 6–15. doi:10.1002/evl3.1
6. Maynard Smith J. What use is sex? J Theor Biol. 1971;30: 319–335. doi:10.1016/0022-5193(71)90058-0
7. Felsenstein J. THE EVOLUTIONARY ADVANTAGE OF RECOMBINATION. Genetics. 1976;78: 737–756. doi:S1090-0233(10)00296-0 [pii]\r10.1016/j.tvjl.2010.09.005 [doi]
8. Dacks J, Roger AJ. The First Sexual Lineage and the Relevance of Facultative Sex. J Mol Evol. 1999;48: 779–83.
9. Kassir Y, Granot D, Simchen G. IME1, a Positive Regulator Gene of Meiosis in S. cerevisiae. Cell. 1988;52: 853–862.
10. Mirzaghaderi G, Hörandl E. The evolution of meiotic sex and its alternatives. Proc R Soc B Biol Sci. 2016;283: 20161221. doi:10.1098/rspb.2016.1221
11. Beukeboom LW, Vrijenhoek RC. Evolutionary genetics and ecology of sperm-dependent

parthenogenesis. J Evol Biol. 1998;11: 755–782. doi:10.1007/s000360050117

12. Engelstädter J. Constraints on the evolution of asexual reproduction. BioEssays. 2008;30: 1138–1150. doi:10.1002/bies.20833

13. Markow TA. Parents Without Partners: Drosophila as a Model for Understanding the Mechanisms and Evolution of Parthenogenesis. G3. 2013;3: 757–762. doi:10.1534/g3.112.005421

14. Fields AT, Feldheim KA, Poulakis GR, Chapman DD. Facultative parthenogenesis in a critically endangered wild vertebrate. Curr Biol. 2015;25: R446–R447. doi:10.1016/j.cub.2015.04.018

15. Chang C-C, Ting C-T, Chang C-H, Fang S, Chang H-Y. The Persistence of Facultative Parthenogenesis in Drosophila albomicans. PLoS One. 2014;9: e113275. doi:10.1371/journal.pone.0113275

16. Groot TVM, Bruins E, Breeuwer JAJ. Molecular genetic evidence for parthenogenesis in the Burmese python, Python molurus bivittatus. Heredity (Edinb). 2003;90: 130–135. doi:10.1038/sj.hdy.6800210

17. Eisman R, Kaufman TC. Cytological Investigation of the Mechanism of Parthenogenesis in Drosophila mercatorum. Fly. 2007;1: 317–329. doi:10.4161/fly.5408

18. Watts PC, Buley KR, Sanderson S, Boardman W, Ciofi C, Gibson R. Parthenogenesis in Komodo dragons. Nature. 2006;444: 1021–1022. doi:10.1038/nature4441021a

19. van der Kooi CJ, Schwander T. Parthenogenesis: Birth of a New Lineage or Reproductive Accident? Curr Biol. 2015;25: R654–R676. doi:10.1016/j.cub.2015.06.055

20. Schwander T, Vuilleumier S, Dubman J, Crespi BJ. Positive feedback in the transition from sexual reproduction to parthenogenesis. Proc R Soc B Biol Sci. 2010;277: 1435–1442. doi:10.1098/rspb.2009.2113

21. Fuyama Y. Genetics of Parthenogenesis in DROSOPHILA MELANOGASTER. I. The Modes

of Diploidization in the Gynogenesis Induced by a Male-Sterile Mutant, ms(3)K81. Genetics. 1986;112: 237–248.

22. Fuyama Y. Genetics of Parthenogenesis in DROSOPHILA MELANOGASTER. II. Characterization of a Gynogenetically Reproducing Strain. Genetics. 1986;114: 495–509.
23. Templeton AR, Carson HL, Sing CF. The population genetics of parthenogenetic strains of Drosophila mercatorum. II. The capacity for parthenogenesis in a natural, bisexual population. Genetics. 1976;82: 527–542.
24. Stalker HD. Parthenogenesis in Drosophila. Genetics. 1954;39: 4–34. doi:10.1086/282095
25. Coyne JA, Orr HA. Speciation. Sunderland, MA: Sinauer Associates; 2004.
26. Sadler PL, Shakes DC. Anucleate Caenorhabditis elegans sperm can crawl, fertilize oocytes and direct anterior-posterior polarization of the 1-cell embryo. Development. 2000;127: 355–366.
27. Cutter AD, Dey A, Murray RL. Evolution of the Caenorhabditis elegans genome. Mol Biol Evol. 2009;26: 1199–1234. doi:10.1093/molbev/msp048
28. Roelens B, Schvarzstein M, Villeneuve AM. Manipulation of karyotype in Caenorhabditis elegans reveals multiple inputs driving pairwise chromosome synapsis during meiosis. Genetics. 2015;201: 1363–1379. doi:10.1534/genetics.115.182279
29. Fierst JL, Willis JH, Thomas CG, Wang W, Reynolds RM, Ahearne TE, et al. Reproductive Mode and the Evolution of Genome Size and Structure in Caenorhabditis Nematodes. PLoS Genet. 2015;11: e1005323. doi:10.1371/journal.pgen.1005323
30. Meneely PM, Farago AF, Kauffman TM. Crossover distribution and high interference for both the X chromosome and an autosome during oogenesis and spermatogenesis in Caenorhabditis elegans. Genetics. 2002;162: 1169–1177.
31. Madl JE, Herman RK. POLYPLOIDS AND SEX DETERMINATION IN CAENORHABDITIS ELEGANS. Genetics. 1979;93: 393–402.

32. Rockman M V., Kruglyak L. Recombinational landscape and population genomics of Caenorhabditis elegans. PLoS Genet. 2009;5: e1000419. doi:10.1371/journal.pgen.1000419

33. Ross JA, Koboldt DC, Staisch JE, Chamberlin HM, Gupta BP, Miller RD, et al. Caenorhabditis briggsae recombinant inbred line genotypes reveal inter-strain incompatibility and the evolution of recombination. PLoS Genet. 2011;7: e1002174. doi:10.1371/journal.pgen.1002174

34. Oegema K, Hyman AA. Cell division. WormBook, ed C elegans Res Community, Wormb. doi:10.1895/wormbook.1.72.1

35. Itono M, Okabayashi N, Morishima K, Fujimoto T, Yoshikawa H, Yamaha E, et al. Cytological Mechanisms of Gynogenesis and Sperm Incorporation in Unreduced Diploid Eggs of the Clonal Loach, Misgurnus anguillicaudatus (Teleostei: Cobitidae). J Exp Zool. 2007;307A: 35–50. doi:10.1002/jez.a

36. Grosmaire M, Launay C, Siegwald M, Brugière T, Estrada-Virrueta L, Berger D, et al. Males as somatic investment in a parthenogenetic nematode. Science. 2019;363: 1210–1213. doi:10.1126/science.aau0099

37. Fopp-Bayat D, Ocalewicz K, Kucinski M, Jankun M, Laczynska B. Disturbances in the ploidy level in the gynogenetic sterlet Acipenser ruthenus. J Appl Genet. 2017;58: 373–380. doi:10.1007/s13353-017-0389-2

38. Goda T, Abu-Daya A, Carruthers S, Clark MD, Stemple DL, Zimmerman LB. Genetic screens for mutations affecting development of Xenopus tropicalis. PLoS Genet. 2006;2: e91. doi:10.1371/journal.pgen.0020091

39. Hiruta C, Nishida C, Tochinai S. Abortive meiosis in the oogenesis of parthenogenetic Daphnia pulex. Chromosom Res. 2010;18: 833–840. doi:10.1007/s10577-010-9159-2

40. Schlön I, Martens K, Van Dijk P, editors. Lost Sex: The evolutionary biology of parthenogenesis. Dordrecht, The Netherlands: Springer; 2009.

41. Severson AF, Ling L, van Zuylen V, Meyer BJ. The axial element protein HTP-3 promotes cohesin loading and meiotic axis assembly in C. elegans to implement the meiotic program of chromosome segregation. Genes Dev. 2009;23: 1763–1778. doi:10.1101/gad.1808809

42. McNally KP, Panzica MT, Kim T, Cortes DB, McNally FJ. A novel chromosome segregation mechanism during female meiosis. Mol Biol Cell. 2016;27: 2576–2589. doi:10.1091/mbc.E16-05-0331

43. Murdy WH, Carson HL. Parthenogenesis in Drosophila mangabeirai Malog. Am Nat. 1959;93: 355–363. doi:10.1086/282095

44. Lamatsch DK, Schmid M, Schartl M. A somatic mosaic of the gynogenetic Amazon molly. J Fish Biol. 2002;60: 1417–1422. doi:10.1006/jfbi.2002.1939

45. Goddard KA, Megwinoff O, Wessner LL, Giaimo F. Confirmation of gynogenesis in Phoxinus eos-neogaeus (Pisces: Cyprinidae). J Hered. 1998;89: 151–157. doi:10.1093/jhered/89.2.151

46. Aldrich JC, Leibholz A, Cheema MS, Ausió J, Ferree PM. A “selfish” B chromosome induces genome elimination by disrupting the histone code in the jewel wasp Nasonia vitripennis. Sci Rep. 2017;7: 42551. doi:10.1038/srep42551

47. Werren JH, Baldo L, Clark ME. Wolbachia: master manipulators of invertebrate biology. Nat Rev Microbiol. 2008;6: 741–751. doi:10.1038/nrmicro1969

48. Yamaki T, Yasuda GK, Wakimoto BT. The deadbeat paternal effect of uncapped sperm telomeres on cell cycle progression and chromosome behavior in Drosophila melanogaster. Genetics. 2016;203: 799–816. doi:10.1534/genetics.115.182436

49. Yasuda GK, Schubiger G, Wakimoto BT. Genetic Characterization of ms(3) K81, a paternal effect gene of Drosophila melanogaster. Genetics. 1995;140: 219–229.

50. Nelson-Rees WA, Hoy MA, Roush RT. Heterochromatinization, chromatin elimination and haploidization in the parahaploid mite Metaseiulus occidentalis (Nesbitt) (Acarina:

Phytoseiidae). Chromosoma. 1980;77: 263–276. doi:10.1007/BF00286052

51. Baker BS. PATERNAL LOSS (PAL): A MEIOTIC MUTANT IN DROSOPHILA MELANOGASTER CAUSING LOSS OF PATERNAL CHROMOSOMES. Genetics. 1975;80: 267–96.

52. Sanei M, Pickering R, Kumke K, Nasuda S, Houben A. Loss of centromeric histone H3 (CENH3) from centromeres precedes uniparental chromosome elimination in interspecific barley hybrids. Proc Natl Acad Sci. 2011;108: E498–E505. doi:10.1073/pnas.1103190108

53. Gibeaux R, Acker R, Kitaoka M, Georgiou G, van Kruijsbergen I, Ford B, et al. Paternal chromosome loss and metabolic crisis contribute to hybrid inviability in Xenopus. Nature. 2018;553: 337–341. doi:10.1038/nature25188

54. Cutter AD, Baird SE, Charlesworth D. High nucleotide polymorphism and rapid decay of linkage disequilibrium in wild populations of Caenorhabditis remanei. Genetics. 2006;174: 901–913. doi:10.1534/genetics.106.061879

55. Dey A, Chan CKW, Thomas CG, Cutter AD. Molecular hyperdiversity defines populations of the nematode Caenorhabditis brenneri. Proc Natl Acad Sci U S A. 2013;110: 11056–60. doi:10.1073/pnas.1303057110

56. Jaquiéry J, Stoeckel S, Larose C, Nouhaud P, Rispe C, Mieuzet L, et al. Genetic Control of Contagious Asexuality in the Pea Aphid. PLoS Genet. 2014;10: e1004838. doi:10.1371/journal.pgen.1004838

57. Kiontke KC, Félix M-A, Ailion M, Rockman M V., Braendle C, Pénigault J-B, et al. A phylogeny and molecular barcodes for Caenorhabditis, with numerous new species from rotting fruits. BMC Evol Biol. 2011;11: 339. doi:10.1186/1471-2148-11-339

58. Stevens L, Félix M-A, Beltran T, Braendle C, Caurcel C, Fausett S, et al. Comparative genomics of 10 new *Caenorhabditis* species. Evol Lett. 2019; 3: 217-236. doi: 10.1002/evl3.110

59. Brenner S. The Genetics of Caenorhabditis elegans. Genetics. 1974;77: 71–94. doi:10.1111/j.1749-6632.1999.tb07894.x

60. Edgar RC. MUSCLE: Multiple sequence alignment with high accuracy and high throughput. Nucleic Acids Res. 2004;32: 1792–1797. doi:10.1093/nar/gkh340

61. Guindon S, Dufayard J-F, Lefort V, Anisimova M, Hordijk W, Gascuel O. New algorithms and methods to estimate maximum-likelihood phylogenies: Assessing the performance of PhyML 3.0. Syst Biol. 2010;59: 307–321. doi:10.1093/sysbio/syq010

62. Lamelza P, Ailion M. Cytoplasmic–Nuclear Incompatibility Between Wild Isolates of Caenorhabditis nouraguensis. G3. 2017;7: 823–834. doi:10.1534/g3.116.037101

63. Collins TJ. ImageJ for microscopy. Biotechniques. 2007;43: S25–S30. doi:10.2144/000112505

64. Palopoli MF, Rockman M V., TinMaung A, Ramsay C, Curwen S, Aduna A, et al. Molecular basis of the copulatory plug polymorphism in Caenorhabditis elegans. Nature. 2008;454: 1019–1022. doi:10.1038/nature07171

65. Robinson JT, Thorvaldsdóttir H, Winckler W, Guttman M, Lander ES, Getz G, et al. Integrative genomics viewer. Nat Biotechnol. 2011;29: 24–26. doi:10.1038/nbt.1754

66. Bhalla N, Dernburg AF. A conserved checkpoint monitors meiotic chromosome synapsis in Caenorhabditis elegans. Science. 2005;310: 1683–6. doi:10.1126/science.1117468

67. Sunnucks P, Hales DF. Numerous transposed sequences of mitochondrial cytochrome oxidase I-II in aphids of the genus Sitobion (Hemiptera: Aphididae). Mol Biol Evol. 1996;13: 510–524.

68. Leggett RM, Clavijo BJ, Clissold L, Clark MD, Caccamo M. NextClip: an analysis and read preparation tool for Nextera Long Mate Pair libraries. Bioinformatics. 2014;30: 566–568.

69. Davis MPA, van Dongen S, Abreu-Goodger C, Bartonicek N, Enright AJ. Kraken: A set of tools for quality control and analysis of high-throughput sequence data. Methods. 2013;63:

41–49.

70. Greenfield P, Duesing K, Papanicolaou A, Bauer DC. Blue: correcting sequencing errors using consensus and context. Bioinformatics. 2014;30: 2723–2732.

71. Simpson JT, Durbin R. Efficient de novo assembly of large genomes using compressed data structures. Genome Res. 2012;22: 549–56.

72. English AC, Richards S, Han Y, Wang M, Vee V, Qu J, et al. Mind the Gap: Upgrading Genomes with Pacific Biosciences RS Long-Read Sequencing Technology. Liu Z, editor. PLoS One. 2012;7: e47768. doi:10.1371/journal.pone.0047768

73. Hunt M, Kikuchi T, Sanders M, Newbold C, Berriman M, Otto TD. REAPR: a universal tool for genome assembly evaluation. Genome Biol. 2013;14: R47. doi:10.1155/2013/108486

74. Li H, Durbin R. Fast and accurate long-read alignment with Burrows–Wheeler transform. Bioinformatics. 2010;26: 589–595. doi:10.1093/bioinformatics/btp698

75. McKenna A, Hanna M, Banks E, Sivachenko A, Cibulskis K, Kernytsky A, et al. The Genome Analysis Toolkit: A MapReduce framework for analyzing next-generation DNA sequencing data. Genome Res. 2010;20: 1297–1303. doi:10.1101/gr.107524.110.20

76. Kajitani R, Toshimoto K, Noguchi H, Toyoda A, Ogura Y, Okuno M, et al. Efficient de novo assembly of highly heterozygous genomes from whole-genome shotgun short reads. Genome Res. 2013;24: 1384–1395. doi:10.1038/nbt.2727

77. Kurtz S, Phillippy A, Delcher AL, Smoot M, Shumway M, Antonescu C, et al. Versatile and open software for comparing large genomes. Genome Biol. 2004;5: R12.

78. Andolfatto P, Davison D, Erezyilmaz D, Hu TT, Mast J, Sunayama-Morita T, et al. Multiplexed shotgun genotyping for rapid and efficient genetic mapping. Genome Res. 2011;21: 610–7. doi:10.1101/gr.115402.110

79. Broman KW, Wu H, Sen S, Churchill GA. R/qtl: QTL mapping in experimental crosses. Bioinformatics. 2003;19: 889–890. doi:10.1093/bioinformatics/btg112

80. Taylor J, Butler D. R Package ASMap: Efficient Genetic Linkage Map Construction and Diagnosis. J Stat Softw. 2017;79: 1–29. doi:10.18637/jss.v079.i06

81. Kent WJ, Baertsch R, Hinrichs A, Miller W, Haussler D. Evolution's cauldron: duplication, deletion, and rearrangement in the mouse and human genomes. Proc Natl Acad Sci U S A. 2003;100: 11484–9. doi:10.1073/pnas.1932072100

82. Laetsch DR, Blaxter ML. BlobTools: Interrogation of genome assemblies. F1000Research. 2017;6: 1287. doi:10.12688/f1000research.12232.1

83. Wu TD, Nacu S. Fast and SNP-tolerant detection of complex variants and splicing in short reads. Bioinformatics. 2010;26: 873–881. doi:10.1093/bioinformatics/btq057

84. Liu Y, Schröder J, Schmidt B. Musket: a multistage k-mer spectrum-based error corrector for Illumina sequence data. Bioinformatics. 2013;29: 308–315. doi:10.1093/bioinformatics/bts690

85. Simão FA, Waterhouse RM, Ioannidis P, Kriventseva E V., Zdobnov EM. BUSCO: Assessing genome assembly and annotation completeness with single-copy orthologs. Bioinformatics. 2015;31: 3210–3212. doi:10.1093/bioinformatics/btv351

86. Hunter SS, Lyon RT, Sarver BAJ, Hardwick K, Forney LJ, Settles ML. Assembly by Reduced Complexity (ARC): a hybrid approach for targeted assembly of homologous sequences. bioRxiv. 2015; 014662. doi: 10.1101/014662. doi:10.1101/014662

87. Dey A, Jeon Y, Wang G-X, Cutter AD. Global population genetic structure of Caenorhabditis remanei reveals incipient speciation. Genetics. 2012;191: 1257–1269. doi:10.1534/genetics.112.140418

88. Li H, Handsaker B, Wysoker A, Fennell T, Ruan J, Homer N, et al. The Sequence Alignment/Map format and SAMtools. Bioinformatics. 2009;25: 2078–2079. doi:10.1093/bioinformatics/btp352

89. Huber W, Carey VJ, Gentleman R, Anders S, Carlson M, Carvalho BS, et al. Orchestrating

high-throughput genomic analysis with Bioconductor. Nat Methods. 2015;12: 115–121. doi:10.1038/nmeth.3252

90. Olshen AB, Venkatraman ES, Lucito R, Wigler M. Circular binary segmentation for the analysis of array-based DNA copy number data. Biostatistics. 2004;5: 557–572. doi:10.1093/biostatistics/kxh008

91. Cutter AD, Jovelin R, Dey A. Molecular hyperdiversity and evolution in very large populations. Mol Ecol. 2013;22: 2074–2095. doi:10.1111/mec.12281

Figure 1

A

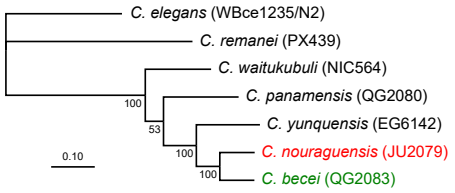

B

cross	viable F1 adults	dead F1 embryos	frequency of viable F1 adults (%)
C. nouraguensis (JU1825) ♀ x *C. becei* (QG711) ♂	5	6239	0.08
C. nouraguensis (NIC59) ♀ x *C. becei* (QG711) ♂	2	5913	0.03
C. nouraguensis (NIC54) ♀ x *C. becei* (QG711) ♂	14	4227	0.33
C. becei (QG711) ♀ x *C. nouraguensis* (JU1825) ♂	0	4530	0
C. becei (QG711) ♀ x *C. nouraguensis* (NIC59) ♂	0	3091	0
C. becei (QG711) ♀ x *C. nouraguensis* (NIC54) ♂	0	4308	0

C

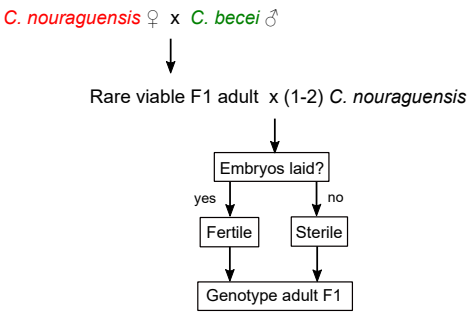

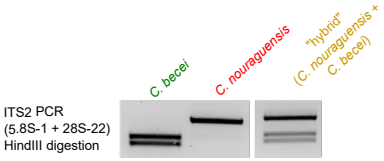

D

C. nouraguensis (JU1825) ♀ x *C. becei* (QG711) ♂

Genotype of F1 adult at W02B12.9 locus (Chr. II)

Fertility of F1 adult	Hybrid (*C. nouraguensis*/*C. becei*)		Maternal (*C. nouraguensis*)		
	female	**male**	**female**	**male**	**total**
Fertile	0	0	7	1	8
Sterile	13	4	1	0	18
total	13	4	8	1	26

C. nouraguensis (NIC54) ♀ x *C. becei* (QG711) ♂

Genotype of F1 adult at ITS2 locus (Chr. I)

Fertility of F1 adult	Hybrid (*C. nouraguensis*/*C. becei*)		Maternal (*C. nouraguensis*)		
	female	**male**	**female**	**male**	**total**
Fertile	0	0	10	0	10
Sterile	21	5	1	0	27
total	21	5	11	0	37

Figure 2

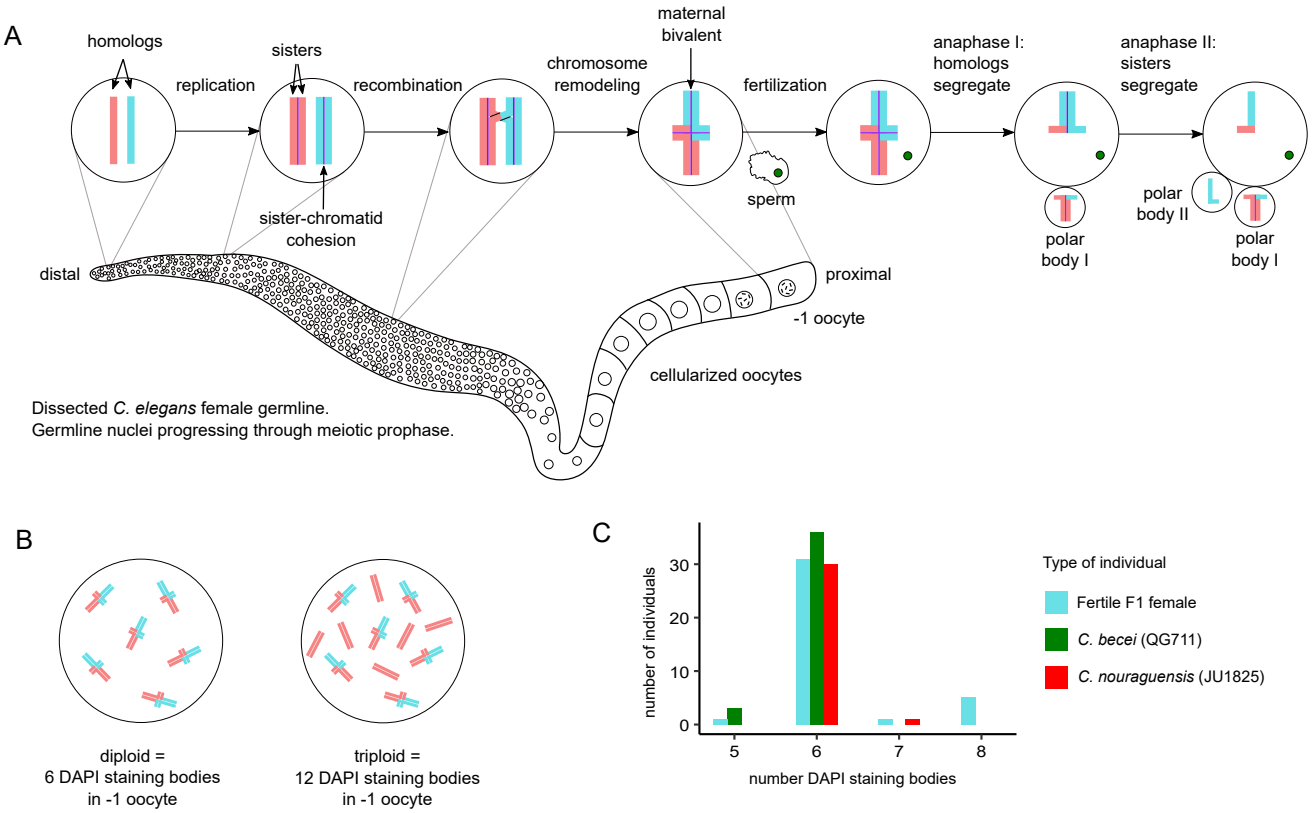
A
homologs
replication
sisters
recombination
chromosome remodeling
maternal bivalent
fertilization
anaphase I: homologs segregate
anaphase II: sisters segregate
sister-chromatid cohesion
sperm
polar body I
polar body II
polar body I
distal
proximal
-1 oocyte
cellularized oocytes
Dissected C. elegans female germline.
Germline nuclei progressing through meiotic prophase.
B
diploid = 6 DAPI staining bodies in -1 oocyte
triploid = 12 DAPI staining bodies in -1 oocyte
C
number of individuals
0
10
20
30
5
6
7
8
number DAPI staining bodies
Type of individual
Fertile F1 female
C. becei (QG711)
C. nouraguensis (JU1825)

Figure 3

A

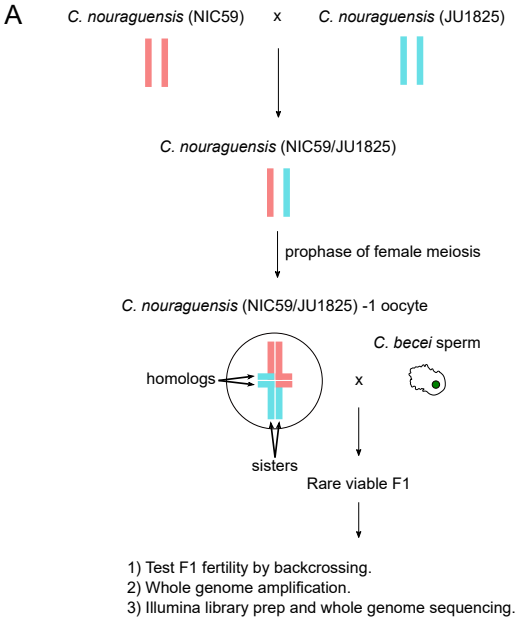

B

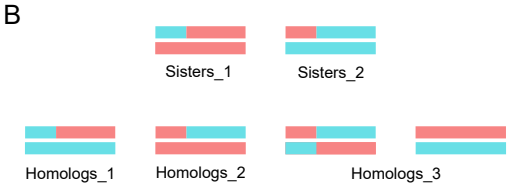

C

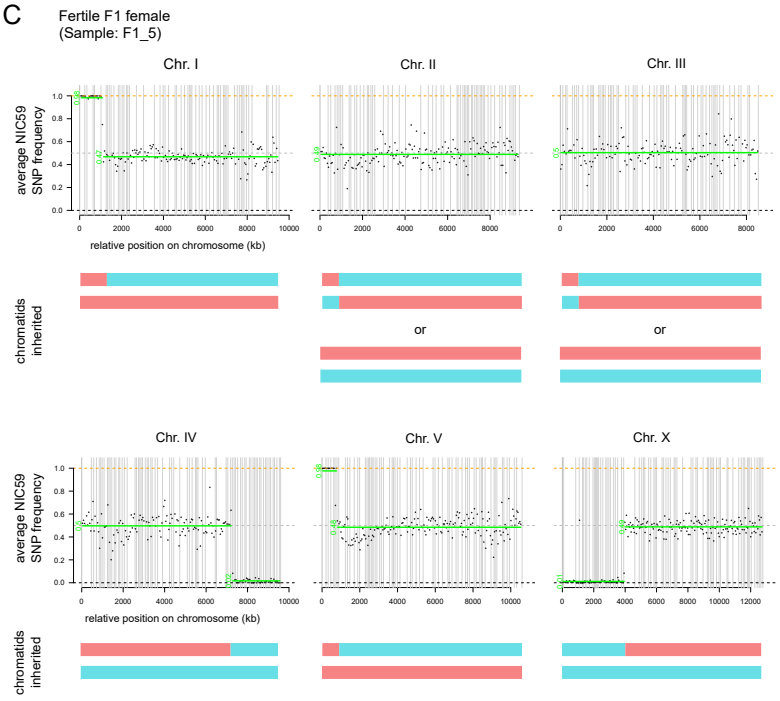

D

	Sisters_1	Sisters_2	Homologs_1	Homologs_2	Homologs_3	total
Observed in combined fertile F1 (10)	0	0	10	10	33	53
Expected if two chromatids randomly inherited	9	9	9	9	18	54
Expected if two homologs randomly inherited	0	0	14	14	28	56

Figure 4

A

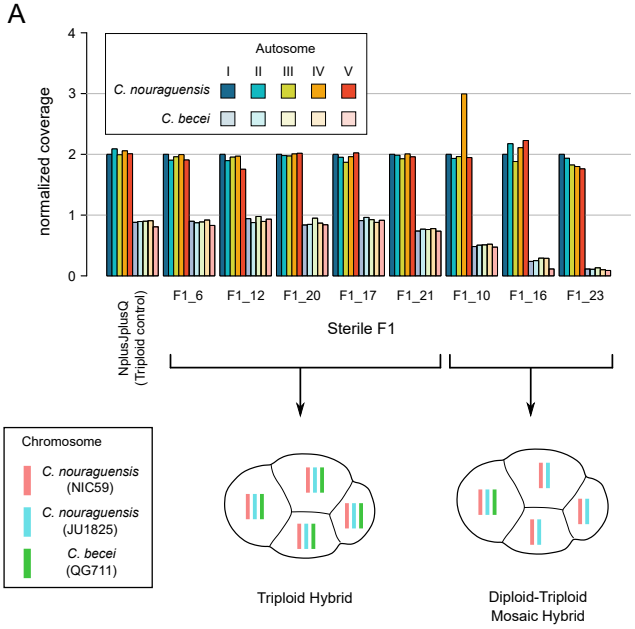

B

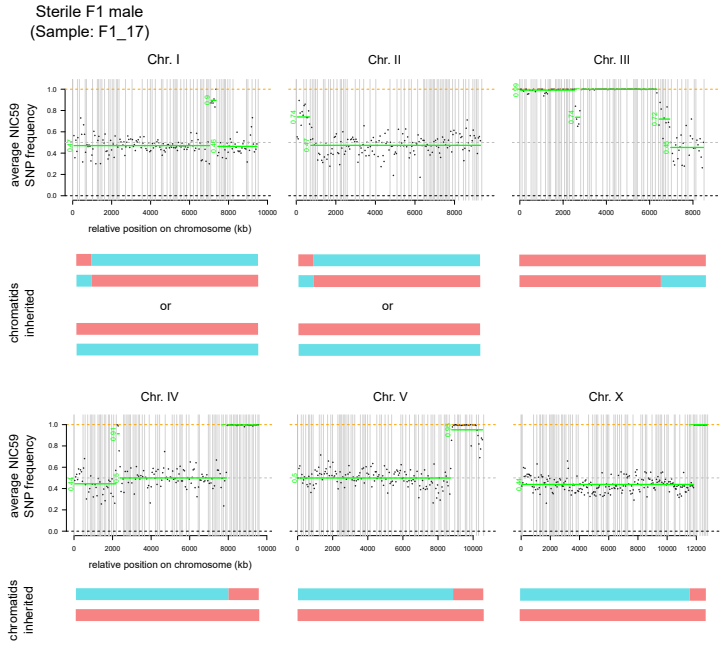

C

	Sisters_1	Sisters_2	Homologs_1	Homologs_2	Homologs_3	total
Observed in combined sterile F1 (8)	1	0	11	13	18	43
Expected if two chromatids randomly inherited	7	7	7	7	14	42
Expected if two homologs randomly inherited	0	0	11	11	22	44

D

	Sisters_1	Sisters_2	Homologs_1	Homologs_2	Homologs_3	total
Observed in combined sterile and fertile F1 (18)	1	0	21	23	51	96
Expected if two chromatids randomly inherited	16	16	16	16	32	96
Expected if two homologs randomly inherited	0	0	24	24	48	96

Figure 5

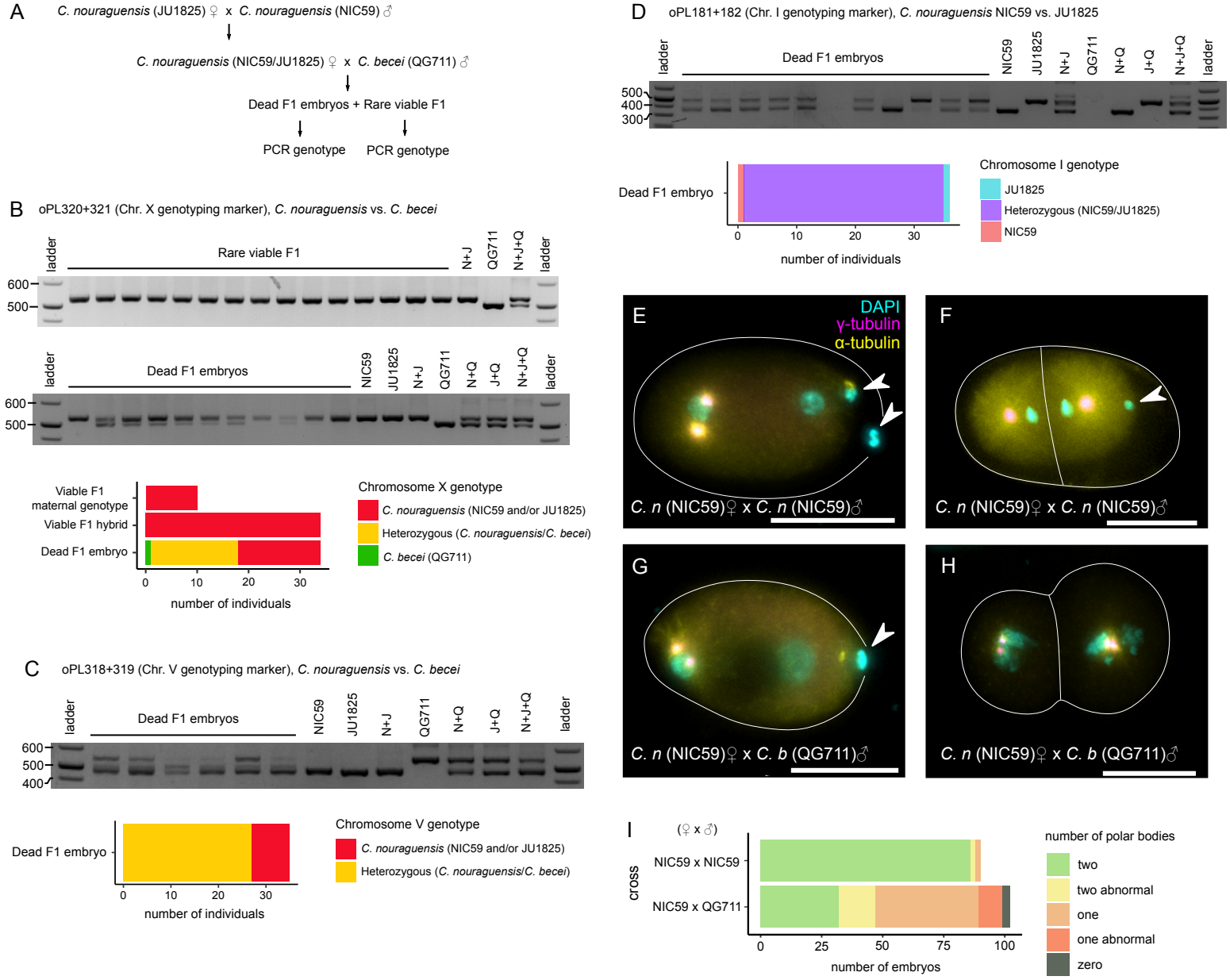
A
C. nouraguensis (JU1825) ♀ x C. nouraguensis (NIC59) ♂
C. nouraguensis (NIC59/JU1825) ♀ x C. becei (QG711) ♂
Dead F1 embryos + Rare viable F1
PCR genotype
PCR genotype
B
oPL320+321 (Chr. X genotyping marker), C. nouraguensis vs. C. becei
ladder
Rare viable F1
N+J
QG711
N+J+Q
ladder
600
500
ladder
Dead F1 embryos
NIC59
JU1825
N+J
QG711
N+Q
J+Q
N+J+Q
ladder
600
500
Viable F1 maternal genotype
Viable F1 hybrid
Dead F1 embryo
0
10
20
30
number of individuals
Chromosome X genotype
C. nouraguensis (NIC59 and/or JU1825)
Heterozygous (C. nouraguensis/C. becei)
C. becei (QG711)
C
oPL318+319 (Chr. V genotyping marker), C. nouraguensis vs. C. becei
ladder
Dead F1 embryos
NIC59
JU1825
N+J
QG711
N+Q
J+Q
N+J+Q
ladder
600
500
400
Dead F1 embryo
0
10
20
30
number of individuals
Chromosome V genotype
C. nouraguensis (NIC59 and/or JU1825)
Heterozygous (C. nouraguensis/C. becei)
D
oPL181+182 (Chr. I genotyping marker), C. nouraguensis NIC59 vs. JU1825
ladder
Dead F1 embryos
NIC59
JU1825
N+J
QG711
N+Q
J+Q
N+J+Q
ladder
500
400
300
Dead F1 embryo
0
10
20
30
number of individuals
Chromosome I genotype
JU1825
Heterozygous (NIC59/JU1825)
NIC59
E
DAPI
γ-tubulin
α-tubulin
C. n (NIC59)♀ x C. n (NIC59)♂
F
C. n (NIC59)♀ x C. n (NIC59)♂
G
C. n (NIC59)♀ x C. b (QG711)♂
H
C. n (NIC59)♀ x C. b (QG711)♂
I
(♀ x ♂)
cross
NIC59 x NIC59
NIC59 x QG711
0
25
50
75
100
number of embryos
number of polar bodies
two
two abnormal
one
one abnormal
zero

Figure 6

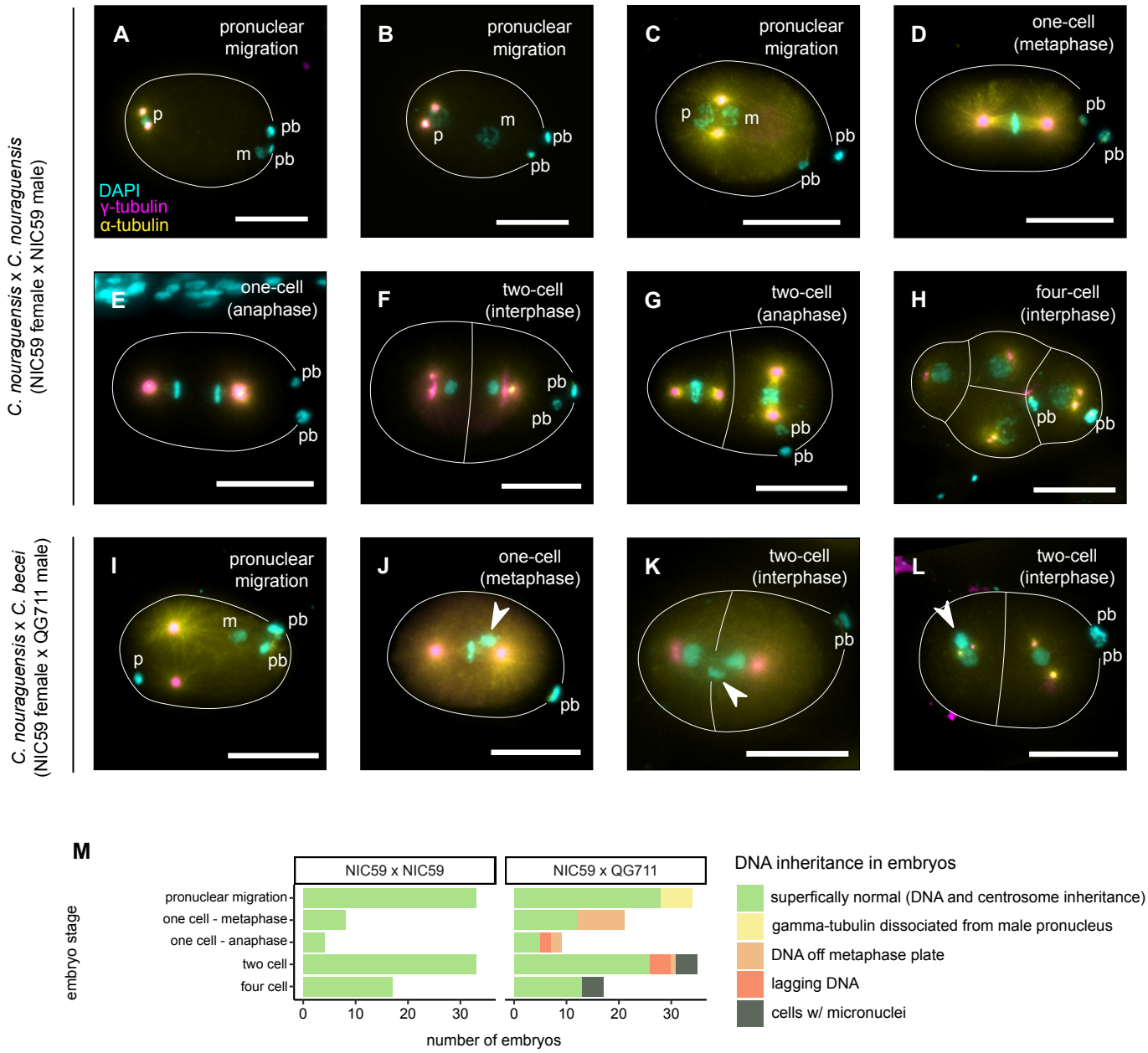
C. nouraguensis x C. nouraguensis
(NIC59 female x NIC59 male)
C. nouraguensis x C. becei
(NIC59 female x QG711 male)
A
pronuclear migration
p
pb
m
pb
DAPI
γ-tubulin
α-tubulin
B
pronuclear migration
m
p
pb
pb
C
pronuclear migration
p
m
pb
pb
D
one-cell (metaphase)
pb
pb
E
one-cell (anaphase)
pb
pb
F
two-cell (interphase)
pb
pb
G
two-cell (anaphase)
pb
pb
H
four-cell (interphase)
pb
pb
I
pronuclear migration
m
pb
p
pb
J
one-cell (metaphase)
pb
K
two-cell (interphase)
pb
L
two-cell (interphase)
pb
pb

M
embryo stage
NIC59 x NIC59
NIC59 x QG711
pronuclear migration
one cell - metaphase
one cell - anaphase
two cell
four cell
0
10
20
30
number of embryos
DNA inheritance in embryos
superfically normal (DNA and centrosome inheritance)
gamma-tubulin dissociated from male pronucleus
DNA off metaphase plate
lagging DNA
cells w/ micronuclei

Figure 7

A

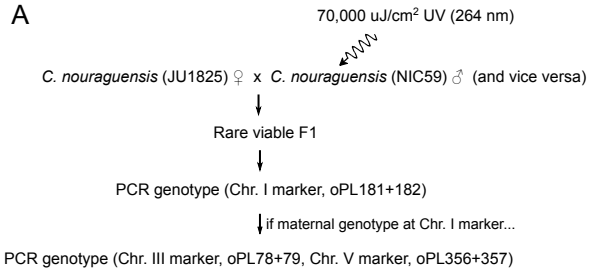

B

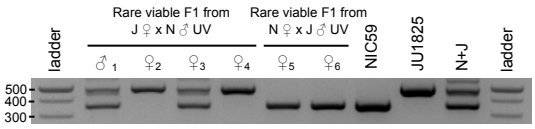

C

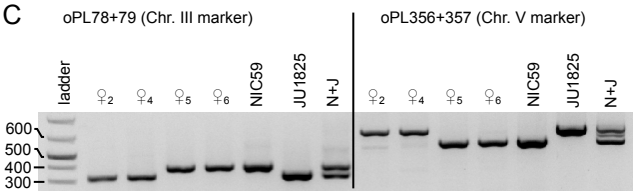

D

cross	Viable F1 w/ maternal genotype at oPL78+79		dead F1 embryos	frequency of gynogenetic offspring (%)
	female	male		
JU1825 ♀ x NIC59 ♂ UV	4	1	~45,000	~0.01
NIC59 ♀ x JU1825 ♂ UV	19	1	~16,000	~0.1

E

-1 oocytes dissected from	# DAPI staining bodies		
	five	six	seven
NIC59 females	2	16	0
Rare F1 females from NIC59 ♀ x JU1825 ♂ UV crosses	3	25	1

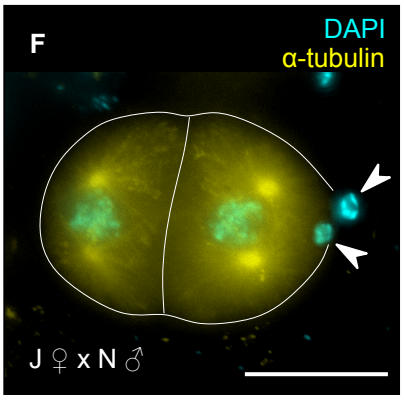

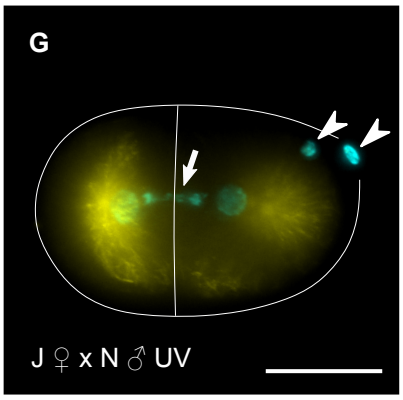

H

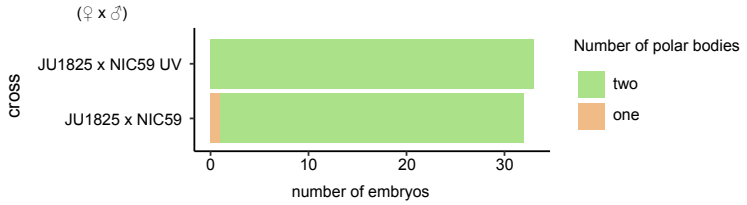

Figure 8

A Normal female meiosis in *C. elegans*

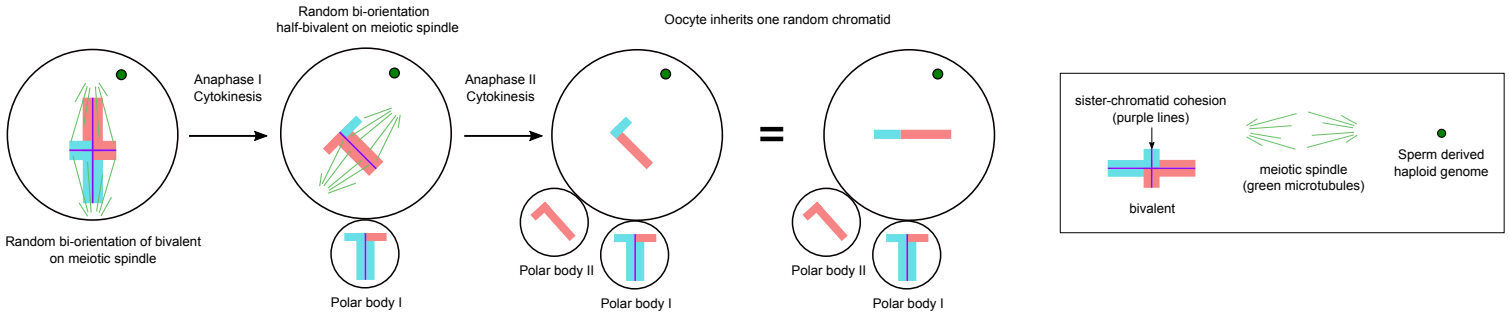
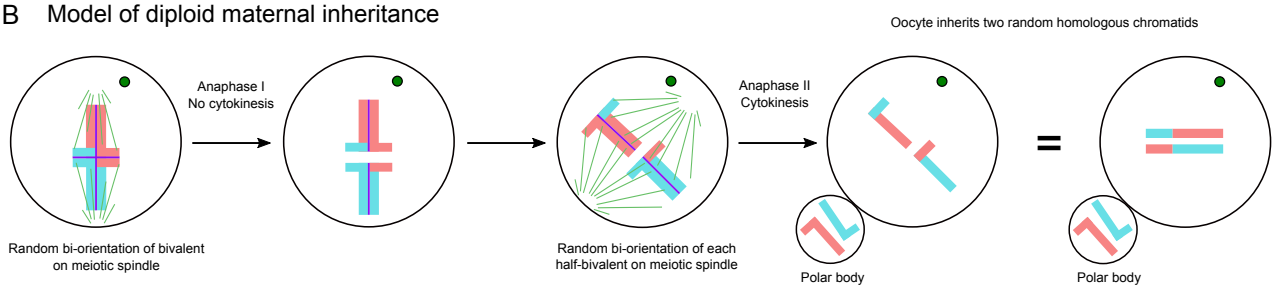
B Model of diploid maternal inheritance